# Modulation by NPYR underlies experience-dependent, sexually dimorphic learning

Sonu Peedikayil-Kurien[1,2], Rizwanul Haque[1,2], Asaf Gat[1,2] and Meital Oren-Suissa[1,2*]

[1] Department of Brain Sciences, Weizmann Institute of Science; Rehovot, 7610001, Israel.

[2] Department of Molecular Neuroscience, Weizmann Institute of Science, Rehovot 7610001, Israel

*Corresponding author. Email: meital.oren@weizmann.ac.il

**Abstract:** The evolutionary paths taken by each sex within a given species sometimes diverge, resulting in behavioral differences. Given their distinct needs, the mechanism by which each sex learns from a shared experience is still an open question. Here, we reveal sexual dimorphism in learning: *C. elegans* males do not learn to avoid the pathogenic bacteria PA14 as efficiently and rapidly as hermaphrodites. Notably, neuronal activity following pathogen exposure was dimorphic: hermaphrodites generate robust representations, while males, in line with their behavior, exhibit contrasting representations. Transcriptomic and behavioral analysis revealed that the neuropeptide receptor *npr-5*, an ortholog of the mammalian NPY receptor, regulates male learning by modulating neuronal activity. Furthermore, we show the dependency of the males' decision-making on their sexual status and demonstrate the pivotal role of *npr-5* as a modulator of incoming sensory cues. Taken together, we portray sex-specific plasticity in behavior toward a shared experience by modulating learning.

## Introduction

Learning facilitates the organism's ability to cope with a changing environment, making it an inherent property of biological neural systems[1]. To adapt to the environment, the organism needs to retain the learning experience and then use the stored information to alter future responses[2]. The synaptic basis of learning and memory has been well established and provides a solid foundation to assess the relationship between experience-dependent learning and survival[3].

Since sexual selection predicts that males and females are subjected to different selection pressures leading to dimorphisms[4,5], it stands to reason that the same would occur for an essential ability such as learning. Consistent with this prediction, several sex-shared traits such as perception and learning have been previously demonstrated to be modulated by the genetic sex[6–12]. It has also been proposed that learning can be a driving force for evolutionary change[13]. Thus, sex-specific evolutionary drives might be in tension with decision-making processes when facing an environmental cue[14,15]. While a significant portion of sex differences in behavior could be attributed to the neurochemical pathway of circulating sex hormones, it has been suggested that behavior is also influenced by other factors, such as life history and sex-specific gene expression[16]. This indicates a bi-directional relationship between sexual identity and the environment, with far-reaching consequences on cognitive abilities, including learning and memory. How sexual identity drives molecular and circuit changes toward a shared experience that intersects with learning and survival is still an open question.

The nematode *C. elegans* has been a useful model for the study of learning and memory at the molecular, cellular, neural circuitry, and behavioral levels[17]. Numerous studies have demonstrated that *C. elegans* is capable of non-associative learning and short-term memory, in addition to associative learning, long-term memory, and sensory integration of conflicting cues[18–22].

The two sexes of *C. elegans* display sexually dimorphic behaviors, such as mechanosensory responses to tail touch, dosage-dependent differences in nociceptive behaviors, and chemoattraction to odors and chemicals. Some of these differences have been mapped to corresponding network changes [8,23,24].

Here, we investigated if and how the genetic sex affects context- and experience-dependent behavioral plasticity when learning a shared environmental cue. We harnessed the well-established model of short-term pathogenic aversive conditioning in *C. elegans* [21,25,26], where hermaphrodites shift their preference from naïve attraction to aversion upon exposure to the pathogenic bacterium

53 *Pseudomonas aeruginosa* (PA14)[25,27]. We show that males are unable to avoid PA14 as efficiently
54 as hermaphrodites after training. This dimorphic avoidance, however, is not due to differences in
55 the immune responses, but due to layered differences in the sensory and subsequent downstream
56 processing. We observed context-dependent learning when exposing the males to hermaphrodites,
57 which altered their behavior towards PA14. Transcriptomic analyses indicate neuromodulatory
58 regulation, with one candidate, *npr-5*, regulating both the learned as well as context-dependent
59 avoidance by modulating sensory responses. We also unravel the importance of tissue-specific
60 sexual identity and decentralized molecular signaling in regulating male responses. Taken
61 together, our work underscores the diverse levels at which sexual identity modulates dimorphic
62 behavioral responses in each sex towards a shared experience.

63 **Aversive olfactory learning is sexually dimorphic**

64 To test whether short-term aversive learning is sexually dimorphic, we separated virgin males and
65 hermaphrodites and subjected them to an acute training paradigm of pathogenic bacterial exposure
66 (PA14 or *Escherichia coli* strain OP50 as control) that lasted 6 hours, followed by a choice-based
67 test (Fig. 1a). We found that while hermaphrodites efficiently avoided PA14 at the end of the 6-
68 hour mark, males did not display learned aversion (Fig. 1b-c). A similar dimorphic response was
69 observed when we tested the learning abilities of the sexes against another pathogenic bacterium,
70 *Staphylococcus aureus*[28,29] (Supplementary Fig. 1a-b). Analogously, when we tested the naïve
71 avoidance by exposing either sex to a lawn of PA14 and scored lawn occupancy after 6-8 hours,
72 males remained within the PA14 lawn while the hermaphrodites' occupancy was minimal
73 (Supplementary Fig. 1c). We speculated that these observed dimorphisms in short-term learning
74 could arise from differences at checkpoints of information processing within the sexes, such as i)
75 immune responses, ii) integration of sensory information, or iii) a deliberately chosen dimorphic
76 outcome to favor a sex-specific need, in a temporal manner.

77 To determine whether the immune system is activated in both sexes, we examined candidate genes
78 from multiple pathways activated during bacterial infection using either real-time qPCR analysis
79 or reporter expression levels[30]. The CUB-domain containing gene F08G5.6[31] and ShK-like toxin
80 gene F49F1.6, mainly activated by the PMK-1 p38 MAPK pathway[32] were elevated in both sexes
81 after exposure to PA14 (Supplementary Fig. 1d-e). The *pmk-1* pathway-independent immune
82 responder *fshr-1*[33,34] and its effector, F01D5.5 [35], another ShK-like toxin gene, were also elevated
83 in both sexes after training (Supplementary Fig. 1f-g). The *pmk-1* independent gene *irg-3* [30,35] was

also elevated in both sexes, but to a lesser extent in males (Supplementary Fig. 1h). In addition, we imaged the activation of the infection responder gene *irg-1*, which has been shown to be dependent on *zip-2,* a transcription factor specifically activated upon PA14 exposure and is independent of *pmk-1* [30]. We found the *irg-1* levels in the anterior gut region of both sexes to be similar (Fig. 1d-e). The similar pathogenic sensitivity was reflected in killing assays conducted to measure PA14 virulence, where both males and hermaphrodites died with similar kinetics (Fig. 1f, Supplementary Fig. 1i). This is in line with the observation that males do indeed avoid PA14, but only after much more extended training periods (Supplementary Fig. 1j-k). Thus, even though the immune response of the males was activated, they were unable to integrate the pathogenicity of PA14 towards learned aversion as rapidly as hermaphrodites.

To evaluate if the avoidance of PA14 is either developmentally timed or inherently dimorphic, we subjected juvenile animals to the same training paradigm as the adult animals (See Methods). We observed that juveniles of both sexes failed to learn and actively preferred PA14 even after training (Supplementary Fig. 1l-n). This suggests that the dimorphic behavior observed in adulthood results from a developmentally mature nervous system[24].

To characterize the impact of sexual identity on the learning axis, we feminized or masculinized specific tissues in hermaphrodites and males, respectively, and subjected them to the learning paradigm (Fig. 1g). When only the nervous system is sex-reversed, hermaphrodites exhibited a dramatic reduction in their learning ability (Fig. 1h-i). Contrary to our expectations, pan-neuronally feminized males failed to learn (Fig. 1j-k), even though the sex reversal shifted the olfactory preferences of feminized males for certain odors[24] (Supplementary Fig. 1o), suggesting that the substrate of learned avoidance is restricted mostly to the nervous system in hermaphrodites, but involves additional systems in males. In the absence of a direct link between neuronal regulation and learning in males, we hypothesized that non-neuronal tissues such as the gut and the germline might affect male learning. Indeed, previous studies have shown the importance of the gut in regulating behavior[36,37], yet feminizing the gut of males was also insufficient to enhance learning in males (Fig. 1j-k). Similar results were obtained when analyzing males with a mutated germline, although germline-mutated hermaphrodites seemed to display dampened avoidance (Supplementary Fig. 1p-q). However, when both the nervous system and the gut were feminized, these males learned to avoid PA14 significantly better than wild-type males

(Fig. 1j-k). Thus, the default male drive is orchestrated by several tissues, and their intercommunication is critical for the evaluation and subsequent response to external stimuli.

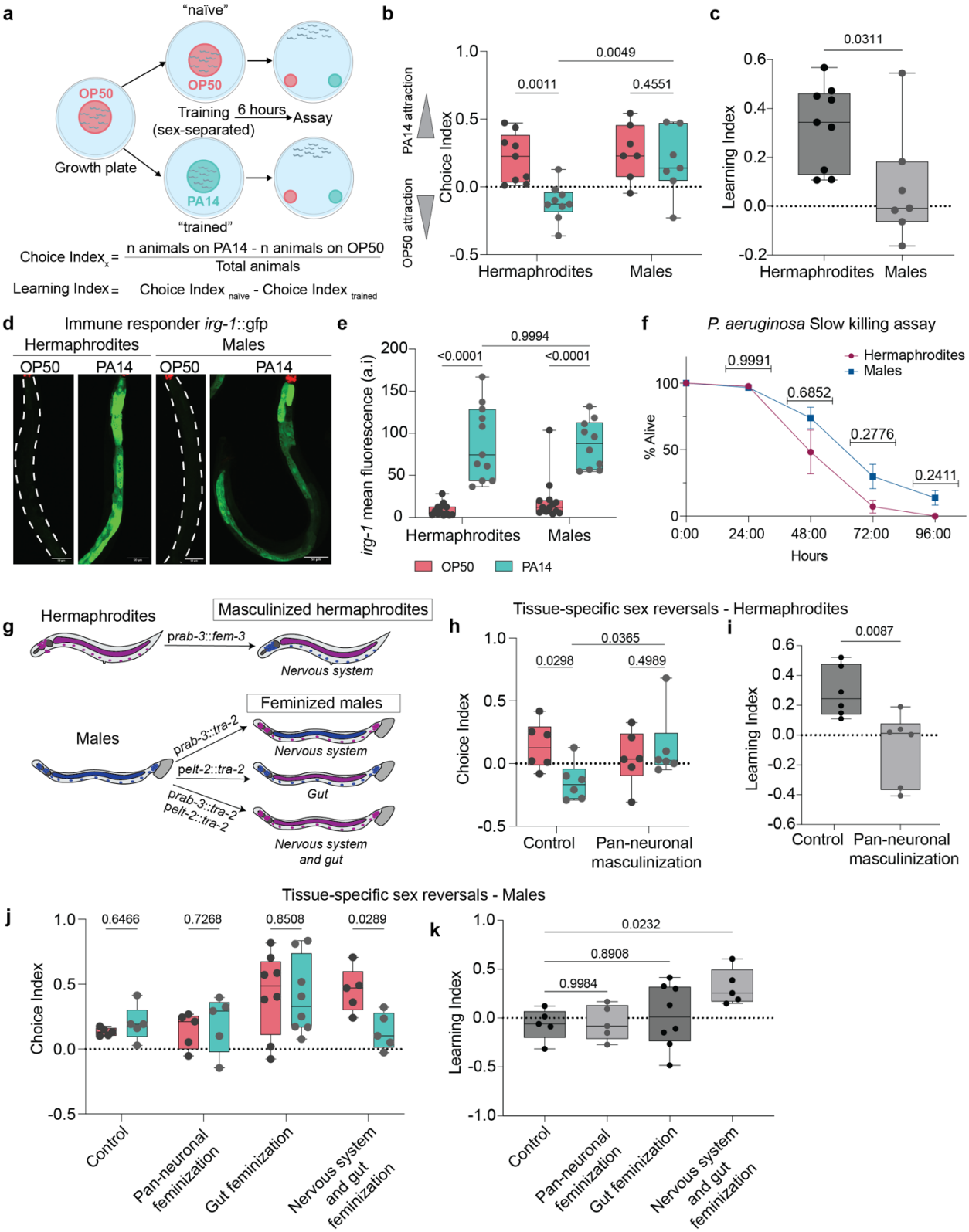

117 Figure 1. **Distinct tissues govern sexually dimorphic short-term learning of PA14 avoidance**
118 **a** Schematic representation of the training paradigm. A group of *C. elegans* was separated into
119 males or hermaphrodites after late L4, exposed to the pathogenic bacterium *Pseudomonas*
120 *aeruginosa* (PA14, cyan, "trained") or OP50 (control, magenta, "naïve") for 6 hours, and then
121 assayed for their choice index against OP50 and PA14 (See Methods). In all figures, n represents
122 the number of animals tested, and N represents the number of biological repeats. **b** The Choice
123 Index of hermaphrodites (OP50, PA14: N = 9) and males (OP50, PA14: N = 7) subjected to the
124 training paradigm in A shows dimorphic responses after training. **c** The learning indices of
125 hermaphrodites (N = 9) and males (N = 7) are dimorphic. **d** Representative confocal micrographs
126 of *irg-1*::GFP hermaphrodites and males trained on OP50 or PA14 after 6 hours of training. Scale
127 bar = 50μm. **e** Quantification of the anterior region of the gut for *irg-1*::GFP in hermaphrodites
128 (OP50: n = 13; PA14: n = 11; n = individual animals) and males (OP50: n = 13; PA14: n = 10; n
129 = individual animals) after exposure to OP50 or PA14. **f** The percentage of live hermaphrodites
130 (N = 6) and males (N = 6) in slow-killing assay. **g** Schematic representation of the tissue sex-
131 reversal experiments (the results of the equivalent germline experiments are presented in
132 Supplementary Fig. 1). **h-i** Choice **(h)** and Learning **(i)** Indices of wild-type (OP50, PA14: N = 6)
133 and pan-neuronally masculinized (p*rab-3*::*fem-3*) hermaphrodites (OP50, PA14: N = 6). **j-k**
134 Choice (**j**) and Learning (**k**) indices of wild-type (control) males (OP50, PA14: N = 5), pan-
135 neuronally feminized (p*rab-3*::*tra-2(ic)*) males (OP50, PA14: N = 5), gut-feminized (p*elt-2*::*tra-*
136 *2(ic)*) males (OP50, PA14: N = 8), and pan-neuronally and gut feminized (p*rab-3*::*tra-2(ic)*;p*elt-*
137 *2*::*tra-2*) males (OP50, PA14, N = 5). Statistical test used are: in (**b**, **e**, **f**, **h**, **j**), a two-way ANOVA
138 with Šídák's multiple comparisons test, in (**c**, **i**), a Mann Whitney test. In (**k**), a Brown-Forsythe
139 and Welch's ANOVA with Dunnett's T3 multiple comparisons test. Box and Whisker plots with
140 mean and entire data range. P values are indicated in the figure.
141

142 **Sexually dimorphic neuronal representations of PA14 exposure**

143 We previously demonstrated that while nociceptive sensory neurons in *C. elegans* respond
144 similarly in the two sexes to a noxious cue (glycerol), the network topology diverges, shaping
145 sexually dimorphic behaviors[8]. The neurons regulating PA14 avoidance have been previously
146 mapped[38,39]. The sensory neuron AWC is required for odor-mediated attraction, while AWB is
147 required for odor-mediated repulsion[40–42]. In addition, these neurons have been recently

established as important in recognizing the odor bouquet presented by PA14 and for regulating both adult and larval learning[35,38,39]. The dimorphic behavior we observed could then arise from distinct computing of environmental cues (i.e., dimorphic neural states lead to dimorphic behavior). To evaluate this, we used calcium imaging to measure the neuronal activity of sensory- and inter-neurons of naïve and trained hermaphrodites and males and quantified the resulting amplitudes during exposure to a sequence of OP50-PA14-OP50 supernatants (see methods). First, we found higher calcium activity in naïve males, upon presentation of PA14, in the sensory neuron AWC (OFF response) (Fig. 2a-b, i, Supplementary Fig. 2a, c, q) and AWB (ON and OFF response) (Fig. 2c-d, j, Supplementary Fig. 2e, g, r-t), compared to naïve hermaphrodites. Next, we examined the change in response after PA14 training. In both sexes, AWC exhibited no change in OFF response after training, compared to naïve animals (Fig. 2a-b, i, Supplementary Fig. 2a-d, q). However, the repellent odor-sensitive AWB displayed distinct dynamics. While there was no change in the ON response of either sex after training (Fig. 2c-d, Supplementary Fig. 2r-s), the OFF response was higher in hermaphrodites (Fig. 2c-d, j, Supplementary Fig. 2t). Taken together, these results suggest that naïve responses in males are stronger in both AWB and AWC, while hermaphrodites showed stronger trained response in AWB (Fig. 2m).

The sensory information from AWC and AWB is passed on to a downstream interneuron AIY, which has been implicated as an information checkpoint that regulates memory retrieval [39,43–45] as well as hermaphrodite training and forgetting states of PA14 aversive learning [26,38]. We observed a reduction in calcium activity after training at the soma of the AIY neuron in both sexes (Fig. 2e-f, k, Supplementary Fig. 2i-l, u). Yet, within the axonal regions of AIY, we observed a decrease in calcium activity after training only in hermaphrodites but not in males (Fig. 2g-h, l, Supplementary Fig. 2x). Interestingly, the latency of calcium responses in AIY soma (Supplementary Fig. 2v) and axonal regions (Supplementary Fig. 2y) of trained males was smaller when compared to trained hermaphrodites, while the time the neuron was active was unchanged in all the groups examined (Supplementary Fig. 2w, z). Taken together, our results show an increased sensory response to PA14 in AWB, and a subsequent decrease in the interneuron AIY only in hermaphrodites. However, the neuronal response landscape was dimorphic with naïve male sensory responses higher and the interneuron AIY displaying compartmentalized (soma vs axonal) dimorphic responses (Fig. 2m).

178 To determine whether the observed dimorphisms in neuronal activity also extend to the synaptic
179 vesicle organization of AIY, i.e., a readout of the learning process, we used a fluorescent readout
180 of RAB-3, which regulates docking of synaptic vesicles[46–48]. The axonal regions of AIY can be
181 distinguished according to their respective synaptic partners as Zone 2 and 3 (Fig. 2n) [48]. We
182 quantified the mCherry expression levels of RAB-3 after training with PA14 and observed a non-
183 dimorphic decrease in RAB-3 levels in both Zones 2 and 3 (Fig. 2o-p), suggesting that the sensory
184 stimulus is processed in both sexes. However, we noticed that the extent of difference in RAB-3
185 expression between the naïve and trained males is lower than that of hermaphrodites (Fig. 2q),
186 suggesting that dimorphic perceptive information is being communicated downstream.

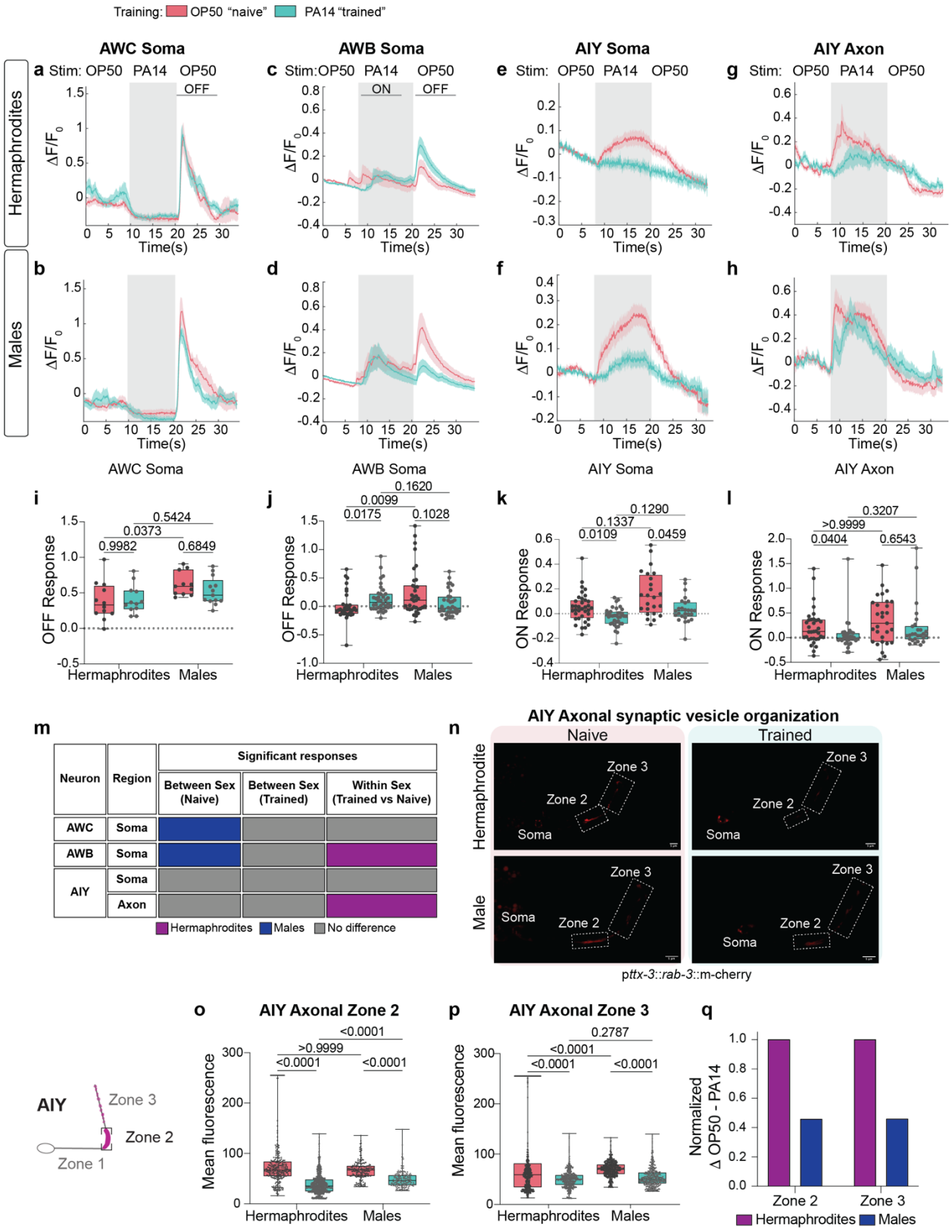


Figure 2. **Distinct dimorphic compartmentalized information processing in response to PA14 stimulus. a-h** From top to bottom, SEM traces of naïve (magenta) and trained (cyan) animals of

both sexes in select neurons. The shaded region in the SEM traces corresponds to the exposure window to PA14 supernatant in both naïve and trained animals. OP50 supernatant was used as the buffer (See Methods). **a** AWC calcium levels in trained (n = 12) and naïve (n = 12) hermaphrodites. **b** AWC calcium levels in trained (n = 13) and naïve (n = 11) males. **c** AWB calcium levels in trained (n = 36) and naïve (n = 34) hermaphrodites. **d** AWB calcium levels in trained (n = 35) and naïve (n = 35) males. **e** AIY soma calcium levels in trained (n = 36) and naïve (n = 34) hermaphrodites. **f** AIY soma calcium levels in trained (n = 35) and naïve (n = 35) males. **g** AIY axonal calcium levels in trained (n = 35) and naïve (n = 35) hermaphrodites. **h** AIY axonal calcium levels in trained (n = 27) and naïve (n = 29) males. **i** Quantification of OFF response of AWC. **j** Quantification of OFF response of AWB. **k** Quantification of ON response of AIY. **l** Quantification of ON response of AIY Axon. **m** Table summarizing the neuronal responses observed. Purple, significant response in hermaphrodites; Blue, Significant response in males; Grey, no difference between the sexes. The sensory neurons AWC and AWB showed higher calcium responses in the naïve males compared to naïve hermaphrodites. After training, hermaphrodites exhibit dimorphic OFF responses in AWB, and ON response in AIY axon. **n** Representative confocal micrographs of p*ttx-3*::*rab-3*::mCherry in naïve and trained hermaphrodites and males showing expression in distinct zones of AIY, namely, a synapse-devoid Zone 1 and synapse-rich Zones 2 and 3. Scale bar = 12μm. **o-p** Synaptic RAB-3 mCherry fluorescence in AIY Zone 2 and Zone 3 axonal regions, respectively. Each dot represents a puncta from 26-47 animals per group. **q** Normalized delta between naïve and trained RAB-3 expression of both sexes in Zone 2 and Zone 3. Hermaphrodites in magenta, and Males in blue. Data is normalized to hermaphrodites. In (**a-h**) change in fluorescence ($\Delta F$) was normalized to the average GCaMP signal in 10 seconds before stimulus start ($F_0$). ON response was defined as the difference in average $\Delta F/ F_0$ during 10 seconds after stimulus start to 5 seconds before stimulus start. OFF response was calculated as the difference in average $\Delta F/ F_0$ during 10 seconds after stimulus removal to 5 seconds before stimulus start. In (**i-l**, **o-p**), the statistical test used is Kruskal-Wallis test with Dunn's multiple comparisons test was performed. Box and Whisker plots with mean and entire data range. P values are indicated in the figure.

**Dimorphic molecular landscape of naïve and trained animals**

220 To characterize the molecular landscape of short-term dimorphic learning, we performed whole-
221 animal transcriptomics on sex-separated naïve and trained animals of both sexes (4 groups with 4
222 biological repeats), and the resultant RNA was sequenced using a bulk optimized protocol of the
223 single-cell MAR-seq protocol[49]. This protocol has been previously used to establish the molecular
224 profile of both sexes in all developmental stages[50]. To visualize the relationship between training
225 and sexual identity across all experimental groups, we performed a principal component analysis
226 (PCA) on the ~ 12,000 identified genes. The PCA revealed a clear separation by sex (Fig. 3a),
227 validated by the dimorphic expression of *lsy-27, tbx-9* and *tra-2* (higher in hermaphrodites[50,51])
228 and *mab-3, pkd-2* and *ins-39* (higher in males[50,52]) (Supplementary Fig. 3a). The training status of
229 the animals was also separated in the PCA (Fig. 3b). We found 869 and 846 differentially
230 expressed genes in hermaphrodites and males, respectively, after training (p value < 0.05;
231 Supplementary Data 1). Unlike the behavioral results, where both naïve and trained males
232 displayed similar attraction towards PA14 (Fig. 1b-c), their molecular landscape differed and
233 reflected the training experience (Fig. 3b). Volcano plots and functional GO term analysis revealed
234 similar changes in immune regulation, fatty acid metabolism, and other stress-related pathways in
235 both sexes, an expected outcome given the gustatory and pathogenic nature of the training
236 bacterium (Fig. 3c-d, Supplementary Fig. 3c, Supplementary Data 1, Supplementary Data 2). Of
237 the entire transcriptomics dataset, 70 genes were previously reported to be involved in PA14-
238 related behaviors (Supplementary Data 2)[26,27,37,39,53–64]. Consistent with our survival assays, most
239 of the genes implicated in PA14 survival, such as *daf-16* and *daf-7*, were non-dimorphic. Genes
240 involved in training and forgetting, such as *gst-38* and *gst-26* [26], were similarly regulated in trained
241 animals of both sexes (Supplementary Fig. 3d, Supplementary Data 2). qPCR analysis of metabolic
242 gene *acdh-1* [65], implicated in PA14 survival, was reduced non-dimorphically after PA14 exposure
243 as indicated by our transcriptomics dataset (Supplementary Fig. 3b, d).
244 To identify transient changes that regulate male learning, we focused on differentially expressed
245 neuro-specific gene classes, such as receptors and neuropeptide families (Fig. 3e, Supplementary
246 Data 2). We uncovered changes in transcription levels for several transcription factors. The
247 homeodomain *ceh-37*, which specifies the identity of the sensory neuron AWB[66] and is involved
248 in regulating immunity from the gut[67] was upregulated in both sexes (Fig. 3e). *mxl-3*, involved in
249 lipolysis and expressed in sensory neurons including ASE, AWC and AWB[68,69] was
250 downregulated in males, while the H3K4 demethylase *rbr-2*, involved in axon guidance and

transmission of stress resistance across generations[70,71] was dimorphically regulated (Fig. 3e). Interestingly, the levels of neuropeptide *ins-11*[61], a negative regulator of PA14 avoidance, were increased in trained animals of both sexes (Fig. 3e), as confirmed by qPCR analysis (Supplementary Fig. 3b, d). *unc-13*, a gene involved in synaptic vesicle clustering, was observed to be dimorphically regulated after training in the sexes, along with the ligand-gated channel *lgc-21* and the neuropeptide receptor *npr-5*. qPCR analysis confirmed the dimorphic expression of *npr-5,* which is down-regulated in males after training (Fig. 3e, Supplementary Fig. 3b), but not of *unc-13* (Supplementary Fig. 3b). Overall, our transcriptomic data suggest that while both sexes respond to PA14 exposure with a similar molecular signature, additional modulatory mechanisms may have evolved to regulate the observed male behavior.

**Sexually dimorphic modulation of the NPY receptor expression**

Recent evidence suggests the importance of integration between the nervous and the immune systems in generating appropriate responses towards pathogenic bacterium[72]. Of note, neuropeptides and their receptors play a major role in PA14 avoidance behavior[73]. One such example is the G-protein coupled receptor *npr-1,* which has been shown to inhibit AQR, PQR, and URX neurons to confer resistance to PA14[74,75]. Given the importance of the neuropeptidergic system in modulating diverse behaviors, including learning[76], the neuropeptide receptor *npr-5* emerged as a likely candidate. Notably, NPR-5 is an ortholog of the mammalian NPY receptor, a key regulator of various behaviors, including learning and memory[77–81]. In *C. elegans*, *npr-5* is involved in regulating foraging and fatty acid metabolism in hermaphrodites[82,83]. In addition, *npr-5* was shown to modulate feeding by regulating the secretion of serotonin from ADF neurons in an NMDAR-dependent manner[84], both of which have independently been implicated in PA14 aversive learning [27,85]. Thus, we sought to examine its role in male learning behavior.

To determine the change in expression post-training, we endogenously tagged *npr-5* using CRISPR-Cas9 gene-editing and quantified its expression levels in head sensory neurons, previously described to regulate behavior[82,83] (Fig. 3f-g). Consistent with previous studies[82], *npr-5* was observed in body wall muscles and multiple neurons, including sensory neurons (Fig. 3f). After training, *npr-5* levels rose in hermaphrodite AWB neurons but were reduced in male AWB neurons (Fig. 3g). Intriguingly, this change in *npr-5* expression resembles the changes in activity levels of AWB (Fig. 2c-d). Although ASJ has been previously described to be involved in

282 processing PA14 experience[37,64,86], and AIY displayed dimorphic response (Fig 2g, h, l), no
283 significant changes were observed in *npr-5* expression after training in ASJ and AIY (Fig. 3g).
284 These results support the transcriptomic data, suggesting *npr-5* is down-regulated in males upon
285 PA14 exposure (Fig. 3e), pointing to a critical role of *npr-5* in modulating learning, perhaps at the
286 sensory level.
287

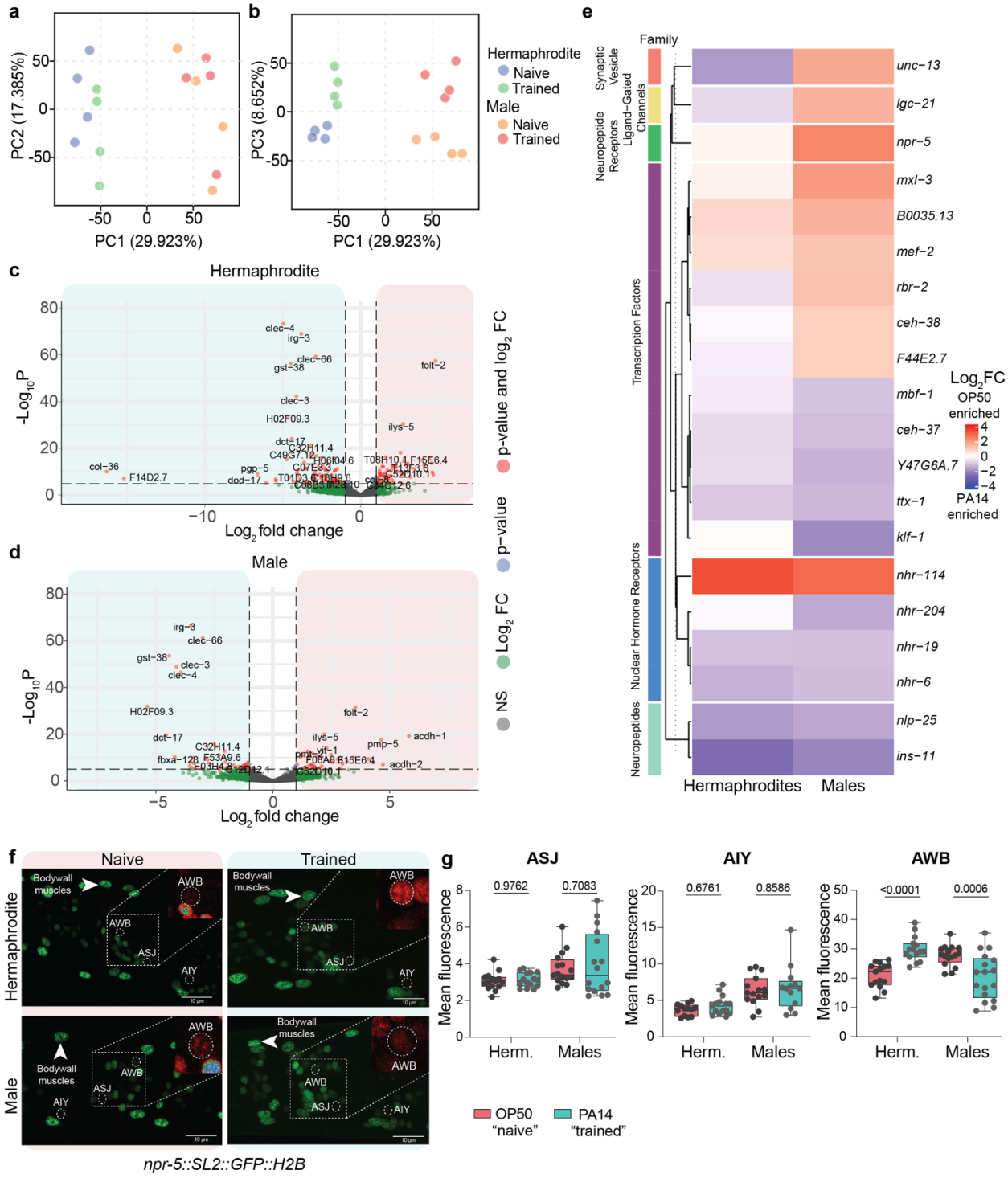


Figure 3. **Sexually dimorphic learning triggers sex-specific changes in NPYR expression. a-b** Principle Component Analysis (PCA) of the transcriptomes of hermaphrodites and males (n = 4 independent samples from 600-800 animals/replicate) after training, ordered according to sex (**a**) and training status (**b**), showing the validity of the data in separating the sexes and training states

293 by transcriptomics. **c-d** Volcano plots of naïve and trained hermaphrodites (**c**) and males (**d**),
294 depicting similar changes in transcripts **e** Heatmap of $\log_2$ fold-change of neuron-relevant genes
295 from naïve vs. trained males (FDR < 0.05) and hermaphrodites. Red indicates enrichment in naïve
296 animals (OP50), while blue indicates enrichment in trained animals (PA14). See also Supplemental
297 tables 1-2. **f** Representative confocal micrographs of *npr-5::SL2::GFP::H2B* CRISPR knock-in in
298 naïve and trained hermaphrodites and males showing expression in body wall muscles and sensory
299 cells. The inset shows the heatmap expression of *npr-5::SL2::GFP::H2B* in the selected region
300 with AWB and ASJ. Scale bar = 10μm. **g** Quantification of mean fluorescent signals of *npr*-5 in
301 ASJ, AIY and AWB, showing dimorphic expression changes in AWB after training (ASJ
302 (hermaphrodites: OP50, PA14 n =15; males: OP50, PA14 n =16); AIY (hermaphrodites: OP50 n
303 =13, PA14 n =15; males: OP50 n =15, PA14 n =13); AWB (hermaphrodites: OP50, PA14 n =15;
304 males: OP50 n =16, PA14 n =17). In **(g)**, statistical test used is two-way ANOVA with Šídák's
305 multiple comparisons test. Box and Whisker plots with mean and entire data range. P values are
306 indicated in the figure.
307
308 **Neuropeptidergic modulation of sex-specific learning**
309 To evaluate the extent of neuropeptidergic regulation in male-specific PA14 aversive learning, we
310 subjected *npr-5* mutants to the training paradigm. Strikingly, males with a partial or full *npr-5*
311 deletion acquired the ability to learn quickly in a similar fashion as wild-type hermaphrodites (Fig.
312 4a-d). Although mutant *npr-5* hermaphrodites still avoided PA14, no significant changes were
313 observed between the naïve and trained responses (Fig. 4a, c). Previous studies[82], along with our
314 calcium imaging (Fig. 2c-d, j) and *npr-5* expression results (Fig. 3f-g) suggest a sensory-specific
315 site-of-action of *npr-5*. Therefore, we rescued *npr-5* expression specifically in AWB (using the
316 *str-1* promoter) and in ciliated neurons (using *tax-4* promoter) in an *npr-5* mutant background.
317 While both manipulations sufficed to impede the decision-making ability as indicated by the
318 choice index (Fig. 4a), reverting the animal back to the wild-type male phenotype, the *tax-4* rescue
319 strain displayed a stronger phenotype in the learning index (Fig. 4b). Thus, *npr-5* is required for
320 suppressing learned avoidance, and its activity, possibly in AWB and other sensory neurons,
321 suggests a sensory gating mechanism in males, in line with the observations made in the neuronal
322 activity of trained males (Fig. 2).

Previous studies have also established the link between various neuropeptides and the regulation of behavioral states[86,87]. Given the dimorphic neuropeptidergic landscape and the decentralized learning processing we observed in males (Fig. 1j-k), we postulated that the learning behavior in males might be regulated by multiple signaling molecules in a molecular network (Supplementary Fig. 4a). Indeed, when we screened select candidate neuropeptides using mutants or RNAi, we observed that several neuropeptides such as *flp-33*, *flp-3* and *flp-18*, a cognate ligand of *npr-5,* were involved (Fig. 4e, Supplementary Fig. 4b-c). The regulation of male PA14 aversive learning by *npr-5* and multiple neuropeptides demonstrates that male learning is an amalgamation of complex internal processing.

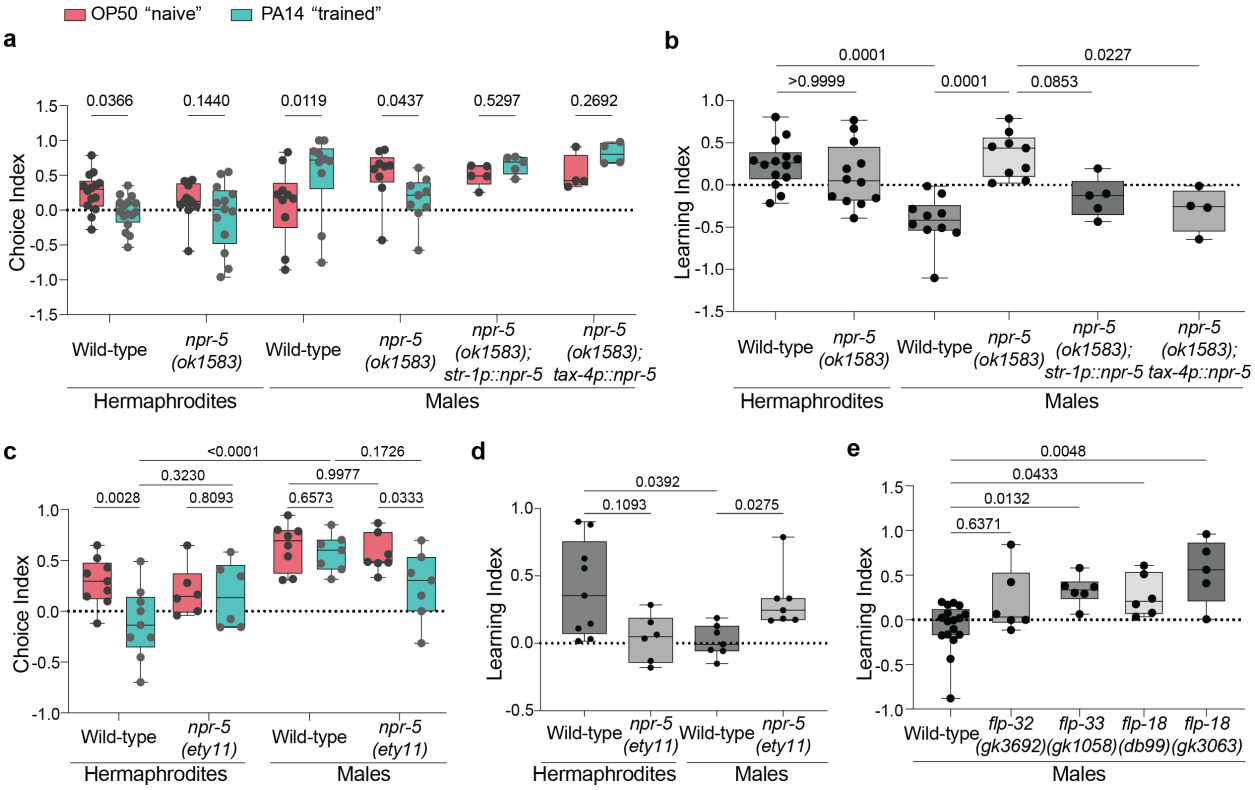


Figure 4**. NPR-5 regulates male-specific behavior. a-b** Choice (**a**) and Learning (**b**) Indices of naïve (magenta) and trained (cyan) wild-type and *npr-5* mutant hermaphrodites and males and male rescue strains where *npr-5* cDNA was expressed either under *str-1* promoter (AWB specific expression [88]) or *tax-4* promoter (expression in ciliated neurons [89]); data shows sex-specific behavioral effects in males (Choice Index: wild-type hermaphrodites: OP50 (N = 12), PA14 (N = 13); *npr-5* hermaphrodites: OP50 (N =10), PA14 (N = 12); wild-type males: OP50, PA14 (N = 10); *npr-5* males: OP50, PA14 (N = 9); p*str-1*::*npr-5*cDNA; *npr-5* males: OP50, PA14 (N = 5); p*tax-4*::*npr-5*cDNA;*npr-5* males: OP50, PA14 (N = 4)). Learning Index: wild-type

341 hermaphrodites: (N = 12); *npr-5* hermaphrodites: (N = 11); wild-type males: (N = 10); *npr-5* males:
342 (N = 9); p*str-1*::*npr-5*cDNA;*npr-5* males: (N = 5); p*tax-4*::*npr-5*cDNA;*npr-5* males: (N = 4)). **c-d**
343 Choice (**c**) and Learning (**d**) indices of naive (magenta) and trained (cyan) wild-type and *npr-5*
344 CRISPR mutant hermaphrodites and males, showing sex-specific behavioral effects in males
345 (hermaphrodites: OP50, PA14, Learning Index (n = 9); *npr-5* hermaphrodites: OP50, PA14,
346 Learning Index (N = 6); males: OP50, PA14, (N = 8), Learning index (N = 7); *npr-5* males: OP50,
347 PA14, Learning Index (N = 7)). **e** Learning indices of wild-type (N = 17), *flp-32* (*gk3692*) mutant,
348 *flp-33* (*gk1058*) mutant, *flp-18* (*db99*) mutant and *flp-18 (gk3063)* males (N = 6), showing
349 peptidergic regulation of male learning. Statistical test used are: in (**a, c**), a two-way ANOVA with
350 Tukey's multiple comparisons test, in **(b, d, e)**, a Kruskal-Wallis test with Dunn's multiple
351 comparisons test. Box and Whisker plots with mean and entire data range. P values are indicated
352 in the figure.
353
354 ***npr-5* functions in AWB to modulate PA14 responses**
355 Based on its sensory responses to PA14 (Fig. 2c-d, j), the observed decrease in *npr-5* expression
356 following training (Fig. 3g), and the change in behavior upon rescue (Fig. 4a), AWB is a likely
357 target of *npr-5* action. We, therefore, measured AWB activity in *npr-5* mutants and observed a
358 striking change in calcium response patterns, namely, a heightened OFF response (Fig. 5a-d,
359 Supplementary Fig. 5a-b), compared to wild-type animals (Fig. 2c-d). In addition, only *npr-5*
360 mutant male AWB neurons exhibited a stronger response to the removal of the PA14 stimulus
361 after training (Fig. 5c-d), similar to wild-type hermaphrodites (Fig. 2c, j). The *npr-5*
362 hermaphrodites showed a decrease in both ON and OFF responses after training (Fig. 5a, c,
363 Supplementary Fig. 5a, c-d). Intriguingly, when stimulated with diluted 2-nonanone, an aversive
364 odor recognized by AWB[90], wild-type animals displayed a non-dimorphic response
365 (Supplementary Fig. 5e, g-h). However, *npr-5* mutants showed higher activation in both sexes
366 when compared to their wild-type counterparts, with *npr-5* males displaying dimorphic heightened
367 activation (Supplementary Fig. 5e-h). Together, our results support the dimorphic inhibitory role
368 of *npr-5* in the proper integration of PA14 signals.
369 Even though we observe no change in *npr-5* expression in AIY (Fig. 3g), we found a stark decline
370 in the AIY soma calcium activity in only naïve, but not trained, *npr-5* mutants (Fig. 5e-g,
371 Supplementary Fig. 6a-b, e) compared to wild-type animals (Fig. 2e, f, k, Supplementary Fig. 2i-

372 l), suggesting that *npr-5* is involved in the recognition and processing of PA14 in the naïve state.
373 Similar observations were made in the axonal responses of AIY to PA14 odor in naïve mutant
374 hermaphrodites and males (Fig. 5h-j, Supplementary Fig. 6c-d, h). In contrast to wild-type males,
375 which retained high activation after training (Fig. 2h, l), mutant males showed reduced activation
376 (Fig. 5h-j, Supplementary Fig. 6c-d, h). The lack of change in responses between the naïve and
377 trained states is also reflected in the latency and the activation time of AIY in mutant animals
378 (Supplementary Fig. 6f-g, i-j). Taken together, these results suggest that *npr-5* plays a crucial role
379 in the integration of PA14 naïve cues in both sexes, but also the trained responses of males. This
380 is highlighted also at the synaptic level where the RAB-3 expression of *npr-5* mutant males
381 displayed an increase in mean fluorescence after training (Fig. 5k), unlike wild-type animals (Fig.
382 2o) and *npr-5* mutant hermaphrodites (Fig. 5k). Thus, exposure to PA14 is processed
383 dimorphically between the sexes, altered partly through modulation by *npr-5* in males.

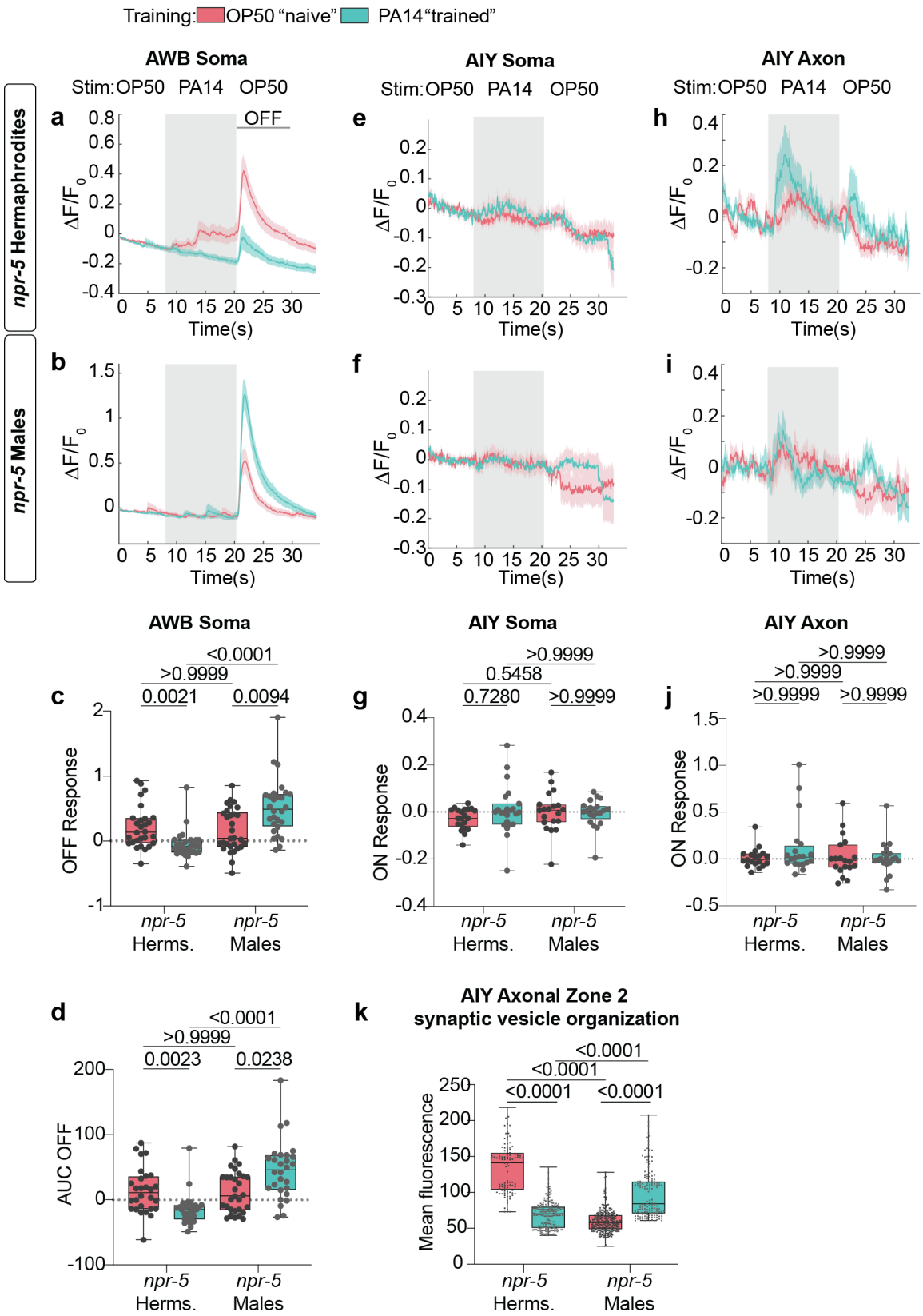
Training: OP50 "naive" PA14 "trained"
AWB Soma
AIY Soma
AIY Axon
Stim: OP50 PA14 OP50
npr-5 Hermaphrodites
npr-5 Males
OFF
ΔF/F0
Time(s)
OFF Response
ON Response
AUC OFF
Mean fluorescence
npr-5 Herms.
npr-5 Males
<0.0001
>0.9999
0.0021
0.0094
0.5458
0.7280
0.0023
0.0238
AIY Axonal Zone 2 synaptic vesicle organization

384

385 Figure 5. **NPR-5 modulates state and sex-specific neuronal activity. a-b, e-f, h-i** From top to
386 bottom, SEM traces of GCaMP signals of select neurons of *npr-5* hermaphrodites and males in
387 naïve (magenta) and trained (cyan) animals. The shaded region corresponds to the exposure
388 window of PA14 supernatant. OP50 supernatant was used as the buffer (See Methods). AWB soma
389 calcium response of naïve and trained **(a)** *npr-5* mutant hermaphrodites (OP50 n = 28, PA14 n =
390 29) and **(b)** *npr-5* mutant males to PA14 supernatant (OP50 n = 30, PA14 n = 28). **c-d**
391 Quantification of **c** the OFF response and **d** AUC of OFF response of AWB. **e** AIY soma calcium
392 levels in naïve (n = 21) and trained (n = 23) *npr-5* mutant hermaphrodites. **f** AIY soma calcium
393 levels in naïve (n = 20) and trained (n = 21) *npr-5* mutant males. **g** Quantification of the ON
394 response of AIY soma. **h** AIY axon calcium levels in naïve (n = 20) and trained (n = 19) *npr-5*
395 mutant hermaphrodites. **i** AIY axon calcium levels in naïve (n = 19) and trained (n = 20) *npr-5*
396 mutant males. **j** Quantification of the ON response of AIY axon. **k** Mean quantification of synaptic
397 *rab-3::mCherry* fluorescence in naïve and trained *npr-5* mutant hermaphrodite and male AIY
398 axon. Each dot represents a puncta from n = 10-17 animals per group. In **(a-b, e-f, h-i)** change in
399 fluorescence was calculated as for Figure 2 (see Methods). In **(c-d, g, j, k)**, statistical test used is
400 Kruskal-Wallis test with Dunn's multiple comparisons test was performed. Box and Whisker plots
401 with mean and entire data range. P values are indicated in the figure.
402
403 **NPR-5 overexpression curbs state-specific male behavior**
404 Our pathogen-sensitivity and calcium-imaging results suggest that while males possess the ability
405 to recognize and potentially process the PA14 experience (Fig. 1c-d, Fig. 2), learning is repressed.
406 *C. elegans* males will abandon food in search of mates[24] and switch from avoidance to attraction
407 of aversive stimuli if hermaphrodites have been experienced[18,91]. Thus, we hypothesized that
408 perhaps repression in our paradigm is a result of the inherent evolutionary drive for mate search.
409 Therefore, diminishing males' sexual drive could lead to PA14 avoidance. To assess this, we
410 trained animals with the other sex ("sex-exposed") or without ("virgin") in the presence of either
411 OP50 or PA14 (Fig. 6a) and checked their choice indices. Sexual conditioning would predict that
412 in the presence of hermaphrodites, the males would be highly attracted to the coupled stimulus, as
413 evidenced by the retention of attraction to OP50 by the naïve hermaphrodite-exposed males (Fig.
414 6b). Surprisingly, we observed that, as opposed to virgin-trained males, which retain their
415 attraction to PA14, trained hermaphrodite-exposed males show decreased attraction to PA14 (Fig.

416 6c). Our results suggest that reducing the males' sexual or mate-searching drive might allow the
417 trained decision-making process to flow uninterrupted. To assess the potential role of *npr-5* in
418 regulating the integration of the internal state into the learning circuit, we overexpressed *npr-5* in
419 sensory neurons of wild-type males to simulate a perpetual 'naïve' state (Fig. 6b). These males
420 failed to avoid PA14, even after training, regardless of their sexual status (Fig. 6c). Taken together,
421 these results suggest that sex-specific needs act as a regulator of male learning, dictated and
422 processed by the inherent neuromodulatory state, where *npr-5* in the sensory neurons of males
423 halts potential learning by modulating the diverse variables that affect male decision-making
424 (Supplementary Fig. 7).

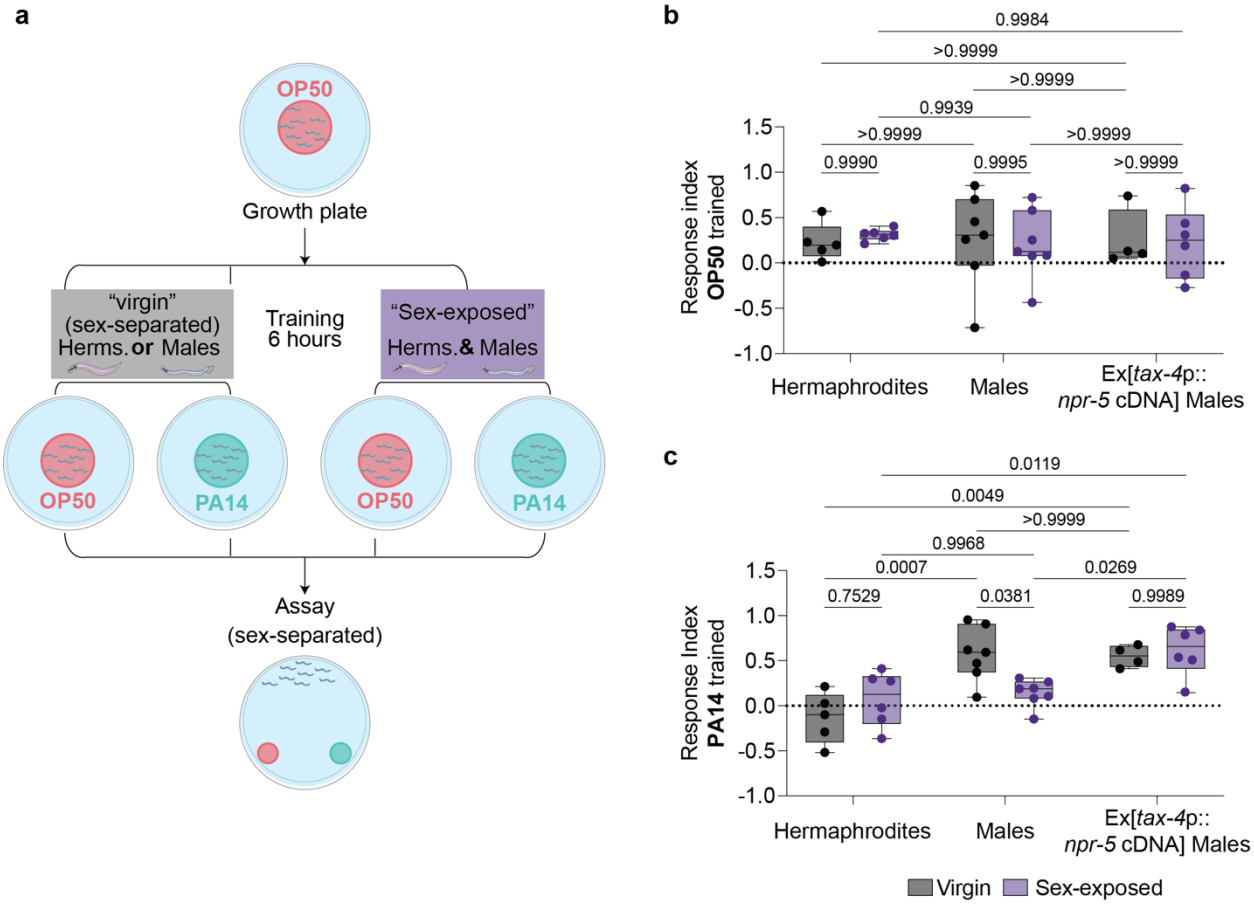


425

426 Figure 6. **The sexual status determines the behavioral outcomes. a** Schematic representation of
427 the conditioning training paradigm. A group of *C. elegans* was separated into males or
428 hermaphrodites after late L4, exposed to OP50 (magenta) or PA14 (cyan) for 6 hours either
429 separately ("virgin") or both sexes together ("sex-exposed"), and then assayed for their choice
430 index against OP50 and PA14 (See Methods). **b** Choice Index of OP50-exposed virgin and sex-

exposed wild-type hermaphrodites (virgin N = 5, sex-exposed N = 6), wild-type males (virgin, sex-exposed N = 7) and *npr-5*-overexpression mutant (p*tax-4*::*npr-5*cDNA) males (virgin N = 4, sex-exposed N = 6). **c** Choice Index of PA14-exposed virgin and sex-exposed wild-type hermaphrodites (virgin N = 5, mated N = 5), wild-type males (virgin N = 7, mated N = 7) and *npr-5*-overexpression males (p*tax-4*::*npr-5*cDNA virgin N = 4, mated N = 6). N refers to number of independent assays with each dot representing a single population assay of 50-200 animals/assay. In (**b**, **c**), statistical test used is two-way ANOVA with Tukey's multiple comparisons test. Box and Whisker plots with mean and entire data range. P values are indicated in the figure.

## Discussion

Sex-specific behaviors have long been recognized as both products and drivers of sexual selection, however learning, a sex-shared trait, would naïvely be expected to withstand the forces of sexual selection, as it is crucial to an organism's survival. Notably, a recent study demonstrated that in a limited information paradigm, female rats outperform males[92]. These findings underscore the importance of evaluating learning within the context of survival, where information is rapid, limited, and temporal. In our study, we investigated the learning performance of both *C. elegans* sexes in a multi-factorial, ethologically relevant paradigm, specifically focusing on pathogen avoidance. Our results reveal an intriguing behavioral dimorphism: Males do not learn to avoid the pathogenic bacteria PA14 as efficiently and rapidly as hermaphrodites.

The exposure to PA14 generates a neural representation of that experience[26,38,39]. Indeed, we observe that two major olfactory neurons, AWC and AWB, and a cholinergic interneuron AIY, reflect that training experience. Consistent with our notion that males can process the training experience, we observe that the soma of AIY reduce its responses to PA14 supernatant, in a manner similar to that of hermaphrodites, while there was no change in AWC after training in either of the sexes. AWB displayed a biphasic response, with naïve males showing higher ON response than naïve hermaphrodites and remained unaffected by training, while the OFF responses of AWB were sexually dimorphic after training. The ON response in AWB could stem from a possible integration mechanism of odors of both OP50 and PA14, a mechanism previously described by Yang et al[90] or it is a response to the removal of OP50[38]. The OFF response of AWB increased in hermaphrodites but reduced in males. Parallelly, the axonal regions of male AIY remain unaffected but that of hermaphrodites showed a reduction analogous with their AIY somas. Although

compartmentalization of information processing has been shown before[93], we uncover a possible sexually dimorphic component. The neuropeptide receptor *npr-5*, maintains these neural states as its mutation caused a switch in male AWB OFF responses, which heightened after training, and a complete silencing of naïve AIY responses. These point to the existence of a sensory gating mechanism in the males where information is diverted, partly through *npr-5*, so as to continue choosing PA14 over OP50 until the repression is alleviated.

Thus, in our investigation of the underlying molecular mechanisms that drive these behavioral disparities, we identified several notable divergences in how males and hermaphrodites process shared information during the learning process (Supplementary Fig. 7). First, learning in hermaphrodites appears to be contingent on their nervous system, whereas males require the combined processing of both their nervous system and gut to make critical choices between benign and pathogenic bacteria. This indicates the existence of a complex regulatory mechanism in males that overrides the immediate threat of infection, a finding in line with recent evidence highlighting the importance of the gut-brain axis in behavior regulation[37,94]. Our study further suggests the presence of a sexually dimorphic component. A potential explanation is the dispersed network of neuropeptides we uncovered that could partially function from the gut. Second, our investigation of neuronal correlates of learning revealed distinct sex-specific activation levels and responses to PA14 stimuli in the sensory neurons and interneurons examined. This observation adds another facet to the developing proposal of the sex differences in synaptic mechanisms that underlie plasticity, learning, and memory[7]. Sex hormones have been shown to play a role in learning[95,96]. Importantly, our study highlights the role genetic sex plays in neuronal function independent of sex hormones. Lastly, the MAR-seq analysis of naïve and trained animals points to transcriptomic differences between males and hermaphrodites, particularly within the underlying neuromodulatory network that potentially contributes to the observed behavioral differences. Similar findings have been reported in butterflies, where a genomic analysis revealed a tissue and gene family-specific bias between the sexes that could explain learning dimorphisms[97]. Recent evidence highlights the important role of neuromodulators in recognizing and avoiding PA14[54,58]. Consistent with this, we demonstrate that the sensory modulation of NPR-5 expression is not only crucial for male behavior but also for the maintenance of neuronal calcium response patterns. Further studies are required to examine this effect in other neurons as well as its universality in multiple behavioral contexts.

493 A key question arises regarding the potential influence of evolutionary pressures. Our data suggest
494 that while males do eventually learn to avoid PA14, they might exhibit short-term repression as a
495 behavioral adaptation. Drawing a parallel to models of foraging animals that exhibit
496 overharvesting or over-staying[98], it may be evolutionarily beneficial for *C. elegans* males to stay
497 in a patch of pathogenic bacterium, despite immunological activation, to maximize the chances of
498 encountering incoming hermaphrodites. Supporting this notion is the observed reduction in
499 attraction towards PA14 in mated males. One interpretation of this finding is that by removing the
500 need to search for mates, the mating pressure is reduced in males, thus allowing them to activate
501 the otherwise gated behavior. This observation is further supported by recent evidence of increased
502 mating by hermaphrodites previously exposed to pathogenic bacterium[99]. It is tempting to
503 speculate that these two pathways could have co-evolved to maximize organismal fitness under
504 dire conditions. In such a scenario, the overall evolutionary demand of the species is fulfilled,
505 albeit in a complex sex-specific manner. A fascinating example is the lower participation of the
506 male bumblebee in cognitive tasks[100], even though they share comparable learning abilities with
507 sterile worker females[101], suggesting that nuanced sex-specific roles alter the perceived learning
508 objective for each sex. Therefore, considering the sex differences in decision-making behavior
509 across organisms, it stands to reason that sexual selection impinges on learning behaviors to favor
510 sex-specific outcomes. By assessing the influence of sexual identity at key levels involved in
511 learning, such as molecular and neuronal circuits, we emphasize the importance of considering sex
512 differences in learning and memory disorders.

513 **Methods**

514 Strains and experimental design

515 Nematodes were cultivated on regular NGM plates on *Escherichia coli* strain OP50 at room
516 temperature unless otherwise mentioned. *him-5*(e1490) were used as a source for wild-type males.
517 All transgenic and bacterial strains are listed in Supplementary Data 3.

518 PA14 aversive learning

519 Animals were age-synchronized by bleaching, unless otherwise specified, and were grown at room
520 temperature on OP50 plates until they were late L4, sex-separated into males and females for
521 behavioral assays as young adults. The training and assay plates were slightly modified from [27].
522 Briefly, OP50 and PA14 were streaked from glycerol stocks onto LB plates and incubated at 37°C

523 overnight. They were then moved to 4°C and used for up to a week. To prepare OP50 or PA14
524 cultures used in the training and assay plates, a small amount of bacteria from streaked plates were
525 incubated in 15 ml tubes containing 5 ml LB at 37°C overnight at 250 rpm. After which, the
526 specified amount of overnight culture (200 µl bacteria for the training plates and 10 µl for the assay
527 plates) was plated onto dried NGM plates and incubated at 37°C overnight and then at 26°C for
528 24 hours. Before being used for behavioral assays, the plates were acclimatized to room
529 temperature (22-23°C). Care was taken to avoid overly dried or contaminated plates. Before each
530 experiment, a test batch of training and assay plates were verified for behavioral consistency using
531 young adult hermaphrodites, failure of which resulted in fresh streaks from a glycerol stock.
532 For the training, sex-separated animals were washed using distilled water or M9 and introduced
533 into training plates for 6 hours at room temperature unless otherwise mentioned. Excess liquid was
534 dried with a Kim-wipe. For the choice assay, the worms were washed off the training plates and
535 washed twice in distilled water or M9. Then, they were placed on the choice assay plates and dried
536 with a Kim-wipe. Once dried, they were left at RT for an hour before being scored manually.
537 Choice Index = $\frac{\#\ worms\ on\ PA14 - \#\ worms\ on\ OP50}{Total\ \#\ worms}$
538 Learning index = Choice $index_{naïve}$ – Choice $index_{trained}$
539 <u>PA14 larval aversive learning</u>
540 To prepare the worms, L1-arrested worms were grown on regular NGM plates until they were L3,
541 approximately 28 hours. For the training, L3 worms were washed and put on either OP50 (control)
542 or PA14 training plates and then incubated at RT for 6 hours. After which, they were washed off
543 the plates and washed twice in distilled water or M9. Then, they were placed on choice assay plates
544 and dried with a Kim-wipe. Once dried, they were left at RT for an hour and then, using a sharp
545 surgical blade, three 1.5cm plugs from the choice areas of the plate were separated as follows:
546 OP50 choice, PA14 choice and Indecision choice (point of insert) and plated onto respective food
547 plates. After 24 hours, the plates were sexed to determine the ratio of each sex in the choice made.
548 <u>Fast-Killing assay</u>
549 The fast killing plates were prepared as described[25]. Briefly, PSG media (Peptone-Glucose-
550 Sorbitol (1% Bacto-Peptone; 1% NaCl; 1% glucose; 0.15M sorbitol; 1.7% Bacto-Agar)) was
551 poured onto 3cm plates and then left to dry. The bacterial cultures were prepared as described
552 above. 10 µl of the overnight culture of PA14 was then used to inoculate the plates and spread
553 evenly using a spreader. The worms were also prepared as described above; sex-separated young

554 adults of each sex (50-80 animals) were introduced to the killing plates and incubated at RT for 21
555 hours; the number of live worms was counted every 6 hours, with dead worms removed from the
556 plates. Once tabulated, the survival percentage was calculated. The assay was done in three
557 technical replicates.

558 Slow-killing assay

559 The slow-killing assay was based on previous methods[25] with slight modifications. The bacterial
560 cultures and plates were prepared as described above, except 20 µl of the overnight culture of
561 PA14 was used to inoculate regular NGM plates and spread evenly using a spreader. Before
562 introducing the worms, 40 µl of 100 mM FUDR was dropped on to the sides of the plate. The
563 worms were prepared as described above, and sex-separated young adults of each sex (40-100
564 animals) were introduced to the killing plates and incubated at RT for 96 hours, during which, the
565 number of live worms was counted every 24 hours, with dead worms removed from the plates.
566 Once tabulated, the survival percentage was calculated. The assay was done in two biological
567 replicates.

568 Lawn-leaving assay

569 The bacterial cultures and plates were prepared as described above, except 30 µl of the overnight
570 culture of OP50 or PA14 inoculum used to inoculate normal 6 cm NGM plates. Next, sex-separated
571 age-synchronized animals were introduced and left at RT for 6-8 hours, and then the number of
572 worms inside or outside the lawn was counted.

573 Chemotaxis Assay

574 Olfactory preference assays for Diacetyl and Pyrazine was conducted as described in [24,40,102], with
575 slight modifications. Animals were sex-separated at late L4s, washed and placed on a 10 cm plate
576 equidistant from two spots of ethanol-diluted odors. After 60 mins, the animals within 1.5 cm of
577 each odor spot was manually counted to achieve the olfactory preference index, OPI = (b-a)/(a+b),
578 where a and b are the two odor spots.

579 Sex-exposed learning assay

580 The assay for the virgin groups was carried out as described above. However, for the mated groups,
581 hermaphrodites were introduced into the training plates at the start of the assay, and at the end of
582 6 hours, the males were separated, and the downstream processing was continued as usual.

583 IRG-1 imaging

584 Age-synchronized animals were incubated on OP50 or PA14 training plates for 6 hours and
585 imaged under a Zeiss LSM 880 confocal microscope at 25x magnification on an agar pad. The
586 PA14 groups were imaged first and the OP50 groups within 8 hours of incubation. Each image file
587 was subjected to the same post processing by converting it to 8-bit image z-projected using
588 maximum intensity and then subtracting background by rolling ball radius of 50 pixels and
589 thresholded between 4-5% before selecting the Region of Interest, which ran from start of the gut
590 until the end of the anterior region, using FIJI and the mean intensity was quantified.

591 AIY Rab-3 mCherry imaging

592 Age-synchronized animals were incubated on OP50 or PA14 training plates for 6 hours and
593 imaged under a Zeiss LSM 880 confocal at 63x magnification on an agar pad. Each image file was
594 subjected to the same post processing by converting it to 8-bit image, z-projected using maximum
595 intensity and then subtracting background using rolling ball radius of 50 and thresholded to
596 generate appropriate mask using analyze particles before selecting the Region of Interest in the red
597 channel for mean intensity quantification. Zone 2 and Zone 3 was identified as previously
598 described [103] and the mean intensity was quantified. To determine the delta between the training
599 states, the males were normalized to the hermaphrodites, with hermaphrodite mean intensity taking
600 a value of one.

601 Calcium imaging

602 Overnight cultures of OP50 and PA14 were centrifuged at 4000g for 10 minutes and the
603 supernatant was then filtered using a 0.22-micron syringe filter. Age-synchronized animals after 6
604 hours of training were used for imaging. Calcium imaging was performed according to Pechuk et
605 al. [8], with changes made to the stimulus type and duration of stimulus. Briefly, the imaging chips
606 were fabricated according to Chronis et al.[103], with the help of the Nanofabrication Unit at the
607 Weizmann Institute of Science. Two pumps control the flow of OP50 supernatant and PA14
608 supernatant into the microfluidic chip. The solutions were channeled through PVC tubes and using
609 a manual switch, the stimulus was presented to the worm, through stainless steel connectors. The
610 pumping rate during experiments was ~0.005 ml/min. The worms were loaded into worm inlet of
611 the chip by using a 1 ml syringe that had worms suspended in OP50 supernatant. 2 min habituation
612 was given prior to imaging with the lasers on. To ensure smooth imaging, 10 mM Levamisole was
613 added to all supernatants and 50 μM rhodamine B was added only to the PA14 supernatant to
614 visualize stimulus delivery. Confocal imaging was done using a 40x magnification water objective.

615 The total imaging duration was 40 sec, constituting 544 frames in total, and the stimulus duration
616 was 12 sec for AWC, 11 sec for AWB, and 15 sec for AIY, after an equal amount of initial time
617 to capture baseline for each neuron respectively. All imaging files were exported as tiff files and
618 the GCaMP fluorescence intensity was analyzed using FIJI. ROIs (regions of interest) of the somas
619 or the axon were drawn manually to best represent the signal, and their mean grey values were
620 quantified (Source Data). Downstream data processing was performed using MATLAB; for each
621 worm, the baseline fluorescent level (F0) was calculated by averaging the mean grey values of 100
622 frames before stimulus delivery, then for each frame, the ΔF was calculated by subtracting F0 from
623 the value of that time point, and the result was divided by F0, to normalize differences in the
624 fluorescence baseline levels between individuals (ΔF/F0). A similar analysis was carried out in the
625 stimulus channel of the images to align the responses to the start of the stimulus (AIY) or the end
626 of the stimulus (AWB and AWC). Once aligned, the ON response was defined as the difference
627 in mean of 10 seconds post stimulus start and the mean of 5 seconds pre-stimulus start. OFF
628 response was defined as the difference in mean of 10 seconds post stimulus stop and the mean of
629 5 seconds pre-stimulus start to keep the baseline for both ON and OFF responses consistent. The
630 latency of the response was defined as the time it took to reach 2 times the SD of the mean before
631 stimulus start. A similar threshold was used to calculate the time of neuronal activity from the start
632 of the stimulus to the end of the recording for each animal.
633 For calcium imaging with 2-nonaone as the stimulus, the same protocol was followed as described
634 above, except that the buffer used was NGM buffer and the stimulus was $10^5$ diluted 2-nonaone.
635 Transcriptomics analysis
636 Approximately 700–1000 animals of each sex were subjected to PA14 or OP50 training for 6 hours
637 and washed with M9 to remove any bacterial remnants. Each training group for each sex had 4
638 biological replicates. The worm pellet was flash-frozen in 500µl TRIzol using liquid nitrogen and
639 stored at -80°C. Total RNA was extracted using the TRIzol LS (Invitrogen) protocol. The RNA
640 from the post isopropanol precipitation step was resuspended in extraction buffer from the
641 PicoPure (Arcturus) RNA isolation kit, and further processing was performed according to the
642 manufacturer's recommendations. After determining the RNA concentration, using a Qubit
643 Fluorometer (model number 4, Invitrogen), and quality, using a Bioanalyzer (Agilent), the samples
644 with a RIN-Score >8 (Supplementary Data 1) were used to create RNA-seq libraries, as previously
645 described using the MARS-seq procedure[49]. The FASTQ files were then processed using the user-

646 friendly transcriptome analysis pipeline (UTAP) (https://utap.wexac.weizmann.ac.il/)[104]. The
647 reads were aligned against the *C. elegans* reference genome WBcel235. The data thus captured
648 was analyzed against the Wormbase database for Gene IDs. Using Python, PCA plots were plotted
649 using seaborn. The data was filtered by sex using the following parameters: Basemean >5 and p-
650 value >0.05 from each sex (naïve vs trained) for all analyses and genes with Basemean >5 was
651 taken ahead for only volcano plots. The p-values for neuronal genes were corrected using the
652 Benjamini-Hochberg method (Supplementary Data 2). The heatmaps and volcano plots were
653 plotted using the Heatmap and EnhancedVolcano functions of R studio (2022.12.0+353),
654 respectively. The resultant data was further taken for GO term analysis of genes from each sex
655 (naïve vs trained) using ShinyGo[105] and the circular barplot was made using ggplot of R studio
656 (2022.12.0+353).

657 RT-PCR

658 Total RNA was extracted for all groups using the protocol described above in 'Transcriptomics
659 analysis'. The isolated RNA was converted to cDNA using random hexamers from the
660 SuperScript™ IV First-Strand Synthesis system. After the concentration was assessed using
661 NanoDrop, qPCR reactions were set up in 10ul reaction mixtures as per manufacturer instructions
662 using Fast SYBR Green Master Mix and the StepOnePlus™ Real-Time PCR system. Ct values
663 were used to quantify the relative expression of the target gene using the $2-\Delta\Delta Ct$ method. *nhr-*
664 *23* was used as the housekeeping gene.

665 Dye staining of *npr-5::GFP* animals

666 Animals at the YA stage were washed with M9 buffer and incubated in 1ml M9 and 5µl DiD dye
667 (Vybrant DiD Cell-labelling solution, ThermoFisher), for 1 hour, on a rotor at ~40 rpm. The worms
668 were then transferred to food plates and the M9 allowed to dry. The animals were then sex-
669 separated and transferred to either OP50 or PA14 training plates and incubated for 6 hours. Next,
670 the worms were transferred to an agar pad and anesthetized with 5µl of 100mM $NaN_3$ and imaged
671 under a Zeiss LSM 880 using a 40x water objective. The Region of Interest was selected in FIJI,
672 using the DiD staining, for the positions of ASJ and AWB, while a co-injection marker was used
673 to assess the position of AIY. The mean intensity was quantified after background correction and
674 thresholding.

675 CRISPR/Cas-9 mediated *npr-5* deletion

676 The CRISPR strategy was based on Paix et al.[106]. Recombinant cas9 (IDT) was injected into N2
677 gonads with tracrRNA (IDT) and three crRNAs, one targeting the dpy-10 locus (Paix et al. 2015)
678 and two flanking the *npr-5* locus (GATAACGTTGCTGATGGTGG, located 52bp downstream of
679 *npr-5* start codon, and GAGACGGGCAAGATGAACAC, located 54bp downstream of stop
680 codon). The repair template was the ssODN
681 CCATTTCGACCATTTCAACCACAACGACTCCCTCCGTTCATCTTGCCCGTCTCTCGAA
682 AAATTCCATTAT, composed of 35nt homology arms from each side of the *npr-5* locus. Rol/dpy
683 F1 progeny were screened by PCR to identify the *npr-5(ety11)* deletion allele. Three primers were
684 included in the reaction: TTCGATGCATGGTTAGTTCG (*npr-5* CR_F1),
685 TTTCCATGTCACTCGTCAGC (*npr-5* CR_R1), GGAAATTCCCGGAAAATGAT (*npr-5*
686 CR_R2), resulting in a 347bp band in WT animals and a 577bp band in ety11 animals.
687 The *syb5786* allele was generated by SunyBiotech.
688 <u>Transgenic strains/molecular cloning</u>
689 The feminization of the gut was generated by expressing *tra-2[intracellular]* under the *elt-2*
690 promoter, cloned by Gibson assembly[90]. *elt-2* promoter was amplified from a plasmid provided by
691 Prof. Sivan Korenblit.
692 To express *npr-5* cDNA specifically in AWB, *npr-5* cDNA was obtained from Genescript and
693 fused to 3.5kb promoter of *str-1* and upstream of SL2::NLS::tagRFP::unc-54 3'UTR using PCR
694 fusion[107].
695 Primers used are in Supplementary Data 3.
696 <u>RNAi</u>
697 RNA interference of select genes was induced using the feeding method [108]. Briefly, L4
698 hermaphrodites were fed HT115 bacteria carrying the dsRNA for the relevant genes including a
699 control empty vector. Multiple plates for each gene were maintained to achieve sufficient young
700 adult males to perform the learning assay as described above. Fresh *pos-1* control was prepared
701 for each RNAi experiment to verify efficiency (Only batches > 95% were used for behavioral
702 assays).
703 <u>Quantification and statistical analysis</u>
704 Each figure legend contains details of the quantification, statistical tests performed and the sample
705 sizes of each individual experiment. All statistical analysis was performed on GraphPad Prism 10.
706

**Acknowledgments**

We thank the members of Oren-Suissa lab for their insights regarding the manuscript. We especially thank Dr. Yehuda Salzberg who helped us in generating the *npr-5* CRISPR strain used in this study. We would like to thank Mario De Bono for furnishing us with much-needed strains. Some strains were provided by the CGC, which is funded by the NIH Office of Research Infrastructure Programs (P40 OD010440). We would also like to thank Prof. Sivan Korenblit for plasmids and Prof. Ravid Straussman for providing us with *S. aureus*. We would like to extend our gratitude to the Nano-Fabrication unit and the Genomics Sandbox unit at the Life Science Core Facility of Weizmann Institute of Science for helping us with the PDMS chips and the transcriptomics, respectively. We thank WormBase, the online database of *C. elegans* genes, for the excellent curation of various information regarding each gene. MOS acknowledges financial support from the European Research Council ERC-2019-STG 850784, Israel Science Foundation grant 961/21, Dr. Barry Sherman Institute for Medicinal Chemistry, Sagol Weizmann-MIT Bridge Program and the Azrieli Foundation. MOS is the incumbent of the Jenna and Julia Birnbach Family Career Development Chair.

**Authors contribution**

SPK conducted and analyzed the experiments. RH performed the library preparation and sequencing for the transcriptomics experiment. AG performed and analyzed the *npr-5* dye staining experiment. MOS supervised and designed the experiments. SPK and MOS wrote the paper.

**Competing interests**

The authors declare no competing interests.

**Data availability**

All data generated and used for analysis are included in the manuscript along with the supplementary information files and Source Data files. The sequence data generated in the study has been deposited in the GEO database under the accession code GSE273091. The RNA-seq data is provided in Supplementary Data 1 and Supplementary Data 2. Quantifications for calcium imaging are added to the Source Data. Raw images for all the imaging experiments can be found at (10.34933/2c05a150-4238-4273-93ec-b419d2c5429f). Source Data are provided in this paper.

**Code availability**

Code generated in this study is available at (10.34933/2c05a150-4238-4273-93ec-b419d2c5429f).

## References


1. Mery, F. Natural variation in learning and memory. *Curr. Opin. Neurobiol.* **23**, 52–56 (2013).

2. Crossley, M., Benjamin, P. R., Kemenes, G., Staras, K. & Kemenes, I. A circuit mechanism linking past and future learning through shifts in perception. *Sci. Adv.* **9**, eadd3403 (2023).

3. Asok, A., Leroy, F., Rayman, J. B. & Kandel, E. R. Molecular Mechanisms of the Memory Trace. *Trends Neurosci.* **42**, 14–22 (2019).

4. Janicke, T., Häderer, I. K., Lajeunesse, M. J. & Anthes, N. Darwinian sex roles confirmed across the animal kingdom. *Sci. Adv.* **2**, e1500983 (2016).

5. Connallon, T. The geography of sex-specific selection, local adaptation, and sexual dimorphism. *Evolution* **69**, (2015).

6. Paletta, P., Bass, N., Aspesi, D. & Choleris, E. Sex Differences in Brain Function and Dysfunction. *Curr Top Behav Neurosci* **62**, 207–234 (2022).

7. Gall, C. M., Le, A. A. & Lynch, G. Sex differences in synaptic plasticity underlying learning. *J. Neurosci. Res.* **101**, 764–782 (2023).

8. Pechuk, V. *et al.* Reprogramming the topology of the nociceptive circuit in C. elegans reshapes sexual behavior. *Curr Biol* (2022) doi:10.1016/j.cub.2022.08.038.

9. Beck, K. D. & Luine, V. N. Evidence for sex-specific shifting of neural processes underlying learning and memory following stress. *Physiol Behav* **99**, 204–211 (2010).

10. Ehmann, B. *et al.* Immature wild orangutans acquire relevant ecological knowledge through sex-specific attentional biases during social learning. *Plos Biol* **19**, e3001173 (2021).

11. Carazo, P., Noble, D. W. A., Chandrasoma, D. & Whiting, M. J. Sex and boldness explain individual differences in spatial learning in a lizard. *Proc Royal Soc B Biological Sci* **281**, 20133275 (2014).

12. Chiu, H. *et al.* A circuit logic for sexually shared and dimorphic aggressive behaviors in Drosophila. *Cell* **184**, 507-520.e16 (2021).

13. Verzijden, M. N. *et al.* The impact of learning on sexual selection and speciation. *Trends Ecol. Evol.* **27**, 511–519 (2012).

14. Møller, A. P. The Behavior of Animals, 2nd Edition. 315–341 (2021) doi:10.1002/9781119109556.ch12.

768 15. Molina-García, L. & Barrios, A. Sex differences in learning—shared principles across taxa.
769 *Curr. Opin. Physiol.* **6**, 65–74 (2018).

770 16. McCarthy, M. M. & Arnold, A. P. Reframing sexual differentiation of the brain. *Nature*
771 *Neuroscience* **14**, 677–683 (2011).

772 17. Rahmani, A. & Chew, Y. L. Investigating the molecular mechanisms of learning and
773 memory using Caenorhabditis elegans. *J. Neurochem.* **159**, 417–451 (2021).

774 18. Sakai, N. *et al.* A sexually conditioned switch of chemosensory behavior in C. elegans. *PLoS*
775 *ONE* **8**, e68676 (2013).

776 19. Ghosh, D. D., Nitabach, M. N., Zhang, Y. & Harris, G. Multisensory integration in C.
777 elegans. *Curr. Opin. Neurobiol.* **43**, 110–118 (2017).

778 20. Stein, G. M. & Murphy, C. T. C. elegans positive olfactory associative memory is a
779 molecularly conserved behavioral paradigm. *Neurobiol. Learn. Mem.* **115**, 86–94 (2014).

780 21. Kaletsky, R. *et al.* C. elegans interprets bacterial non-coding RNAs to learn pathogenic
781 avoidance. *Nature* **586**, 445–451 (2020).

782 22. Sasakura, H. & Mori, I. Behavioral plasticity, learning, and memory in C. elegans. *Curr.*
783 *Opin. Neurobiol.* **23**, 92–99 (2013).

784 23. Setty, H. *et al.* Sexually dimorphic architecture and function of a mechanosensory circuit in
785 C. elegans. *Biorxiv* 2022.02.18.481005 (2022) doi:10.1101/2022.02.18.481005.

786 24. Ryan, D. A. *et al.* Sex, age, and hunger regulate behavioral prioritization through dynamic
787 modulation of chemoreceptor expression. *Curr Biol* **24**, 2509–2517 (2014).

788 25. Tan, M.-W., Mahajan-Miklos, S. & Ausubel, F. M. Killing of Caenorhabditis elegans by
789 Pseudomonas aeruginosa used to model mammalian bacterial pathogenesis. *Proc National Acad*
790 *Sci* **96**, 715–720 (1999).

791 26. Liu, H. *et al.* Forgetting generates a novel state that is reactivatable. *Sci Adv* **8**, eabi9071
792 (2022).

793 27. Zhang, Y., Lu, H. & Bargmann, C. I. Pathogenic bacteria induce aversive olfactory learning
794 in Caenorhabditis elegans. *Nature* **438**, 179–184 (2005).

795 28. Irazoqui, J. E. *et al.* Distinct Pathogenesis and Host Responses during Infection of C. elegans
796 by P. aeruginosa and S. aureus. *PLoS Pathog.* **6**, e1000982 (2010).

797 29. Otarigho, B., Butts, A. F. & Aballay, A. Neuronal NPR-15 modulates molecular and
798 behavioral immune responses via the amphid sensory neuron-intestinal axis in C. elegans. *eLife*
799 **12**, RP90051 (2024).

800 30. Estes, K. A., Dunbar, T. L., Powell, J. R., Ausubel, F. M. & Troemel, E. R. bZIP
801 transcription factor zip-2 mediates an early response to Pseudomonas aeruginosa infection in
802 Caenorhabditis elegans. *Proc National Acad Sci* **107**, 2153–2158 (2010).

803 31. JebaMercy, G. & Balamurugan, K. Effects of sequential infections of Caenorhabditis elegans
804 with Staphylococcus aureus and Proteus mirabilis. *Microbiol. Immunol.* **56**, 825–835 (2012).

805 32. Troemel, E. R. *et al.* p38 MAPK Regulates Expression of Immune Response Genes and
806 Contributes to Longevity in C. elegans. *PLoS Genet.* **2**, e183 (2006).

807 33. Powell, J. R., Kim, D. H. & Ausubel, F. M. The G protein-coupled receptor FSHR-1 is
808 required for the Caenorhabditis elegans innate immune response. *Proc. Natl. Acad. Sci.* **106**,
809 2782–2787 (2009).

810 34. Miller, E. V., Grandi, L. N., Giannini, J. A., Robinson, J. D. & Powell, J. R. The Conserved
811 G-Protein Coupled Receptor FSHR-1 Regulates Protective Host Responses to Infection and
812 Oxidative Stress. *PLoS ONE* **10**, e0137403 (2015).

813 35. Prakash, D. *et al.* 1-Undecene from Pseudomonas aeruginosa is an olfactory signal for flight-
814 or-fight response in Caenorhabditis elegans. *Embo J* **40**, e106938 (2021).

815 36. O'Donnell, M. P., Fox, B. W., Chao, P.-H., Schroeder, F. C. & Sengupta, P. A
816 neurotransmitter produced by gut bacteria modulates host sensory behaviour. *Nature* **583**, 415–
817 420 (2020).

818 37. Singh, J. & Aballay, A. Intestinal infection regulates behavior and learning via
819 neuroendocrine signaling. *Elife* **8**, e50033 (2019).

820 38. Ha, H. *et al.* Functional organization of a neural network for aversive olfactory learning in
821 Caenorhabditis elegans. *Neuron* **68**, 1173–1186 (2010).

822 39. Jin, X., Pokala, N. & Bargmann, C. I. Distinct Circuits for the Formation and Retrieval of an
823 Imprinted Olfactory Memory. *Cell* **164**, 632–643 (2016).

824 40. Bargmann, C. I., Hartwieg, E. & Horvitz, H. R. Odorant-selective genes and neurons mediate
825 olfaction in C. elegans. *Cell* **74**, 515–527 (1993).

826 41. Troemel, E. R., Kimmel, B. E. & Bargmann, C. I. Reprogramming Chemotaxis Responses:
827 Sensory Neurons Define Olfactory Preferences in C. elegans. *Cell* **91**, 161–169 (1997).

828 42. Zhang, Y. Neuronal mechanisms of Caenorhabditis elegans and pathogenic bacteria
829 interactions. *Curr. Opin. Microbiol.* **11**, 257–261 (2008).

830 43. Hawk, J. D. *et al.* Integration of Plasticity Mechanisms within a Single Sensory Neuron of
831 C. elegans Actuates a Memory. *Neuron* **97**, 356-367.e4 (2018).

832 44. Chandra, R. *et al.* Sleep is required to consolidate odor memory and remodel olfactory
833 synapses. *Cell* **186**, 2911-2928.e20 (2023).

834 45. Satoh, Y. *et al.* Regulation of Experience-Dependent Bidirectional Chemotaxis by a Neural
835 Circuit Switch in Caenorhabditis elegans. *J. Neurosci.* **34**, 15631–15637 (2014).

836 46. Hendi, A., Kurashina, M. & Mizumoto, K. Intrinsic and extrinsic mechanisms of synapse
837 formation and specificity in C. elegans. *Cell. Mol. Life Sci.* **76**, 2719–2738 (2019).

838 47. Richmond, J. E. & Broadie, K. S. The synaptic vesicle cycle: exocytosis and endocytosis in
839 Drosophila and C. elegans. *Curr. Opin. Neurobiol.* **12**, 499–507 (2002).

840 48. Colón-Ramos, D. A., Margeta, M. A. & Shen, K. Glia promote local synaptogenesis through
841 UNC-6 (netrin) signaling in C. elegans. *Science* **318**, 103–106 (2007).

842 49. Jaitin, D. A. *et al.* Massively parallel single-cell RNA-seq for marker-free decomposition of
843 tissues into cell types. *Science* **343**, 776–779 (2014).

844 50. Haque, R. *et al.* Sex-specific developmental gene expression atlas unveils dimorphic gene
845 networks in C. elegans. *Nat. Commun.* **15**, 4273 (2024).

846 51. Okkema, P. G. & Kimble, J. Molecular analysis of tra-2, a sex determining gene in
847 C.elegans. *EMBO J.* **10**, 171–176 (1991).

848 52. Barr, M. M. & Sternberg, P. W. A polycystic kidney-disease gene homologue required for
849 male mating behaviour in C. elegans. *Nature* **401**, 386–389 (1999).

850 53. Kawli, T. & Tan, M.-W. Neuroendocrine signals modulate the innate immunity of
851 Caenorhabditis elegans through insulin signaling. *Nat Immunol* **9**, 1415–1424 (2008).

852 54. Yu, Y., Zhi, L., Guan, X., Wang, D. & Wang, D. FLP-4 neuropeptide and its receptor in a
853 neuronal circuit regulate preference choice through functions of ASH-2 trithorax complex in
854 Caenorhabditis elegans. *Sci Rep-uk* **6**, 21485 (2016).

855 55. Deng, P. *et al.* Mitochondrial UPR repression during Pseudomonas aeruginosa infection
856 requires the bZIP protein ZIP-3. *Proc National Acad Sci* **116**, 6146–6151 (2019).

857 56. Wu, T. *et al.* Pheromones Modulate Learning by Regulating the Balanced Signals of Two
858 Insulin-like Peptides. *Neuron* **104**, 1095-1109.e5 (2019).

859 57. Zheng, Z. *et al.* GABAergic synapses suppress intestinal innate immunity via insulin
860 signaling in Caenorhabditis elegans. *Proc National Acad Sci* **118**, e2021063118 (2021).

861 58. Marquina-Solis, J. *et al.* Peptidergic signaling controls the dynamics of sickness behavior in
862 Caenorhabditis elegans. *Biorxiv* 2022.04.16.488560 (2022) doi:10.1101/2022.04.16.488560.

863 59. Chang, H. C., Paek, J. & Kim, D. H. Natural polymorphisms in C. elegans HECW-1 E3
864 ligase affect pathogen avoidance behaviour. *Nature* **480**, 525–529 (2011).

865 60. Chen, Z. *et al.* Two Insulin-like Peptides Antagonistically Regulate Aversive Olfactory
866 Learning in C. elegans. *Neuron* **77**, 572–585 (2013).

867 61. Lee, K. & Mylonakis, E. An Intestine-Derived Neuropeptide Controls Avoidance Behavior
868 in Caenorhabditis elegans. *Cell Reports* **20**, 2501–2512 (2017).

869 62. Cao, X., Kajino-Sakamoto, R., Doss, A. & Aballay, A. Distinct Roles of Sensory Neurons in
870 Mediating Pathogen Avoidance and Neuropeptide-Dependent Immune Regulation. *Cell Reports*
871 **21**, 1442–1451 (2017).

872 63. Zhang, X. & Zhang, Y. DBL-1, a TGF-β, is essential for Caenorhabditis elegans aversive
873 olfactory learning. *Proc National Acad Sci* **109**, 17081–17086 (2012).

874 64. Meisel, J. D., Panda, O., Mahanti, P., Schroeder, F. C. & Kim, D. H. Chemosensation of
875 Bacterial Secondary Metabolites Modulates Neuroendocrine Signaling and Behavior of
876 C. elegans. *Cell* **159**, 267–280 (2014).

877 65. Dasgupta, M. *et al.* NHR-49 Transcription Factor Regulates Immunometabolic Response and
878 Survival of Caenorhabditis elegans during Enterococcus faecalis Infection. *Infect. Immun.* **88**,
879 e00130-20 (2020).

880 66. Lanjuin, A., VanHoven, M. K., Bargmann, C. I., Thompson, J. K. & Sengupta, P. Otx/otd
881 Homeobox Genes Specify Distinct Sensory Neuron Identities in C. elegans. *Dev. Cell* **5**, 621–
882 633 (2003).

883 67. Liu, F. *et al.* The homeodomain transcription factor CEH-37 regulates PMK-1/p38 MAPK
884 pathway to protect against intestinal infection via the phosphatase VHP-1. *Cell. Mol. Life Sci.* **80**,
885 312 (2023).

886 68. O'Rourke, E. J. & Ruvkun, G. MXL-3 and HLH-30 transcriptionally link lipolysis and
887 autophagy to nutrient availability. *Nat. Cell Biol.* **15**, 668–676 (2013).

888 69. Hammarlund, M., Hobert, O., Miller, D. M. & Sestan, N. The CeNGEN Project: The
889 Complete Gene Expression Map of an Entire Nervous System. *Neuron* **99**, 430–433 (2018).

890 70. Mariani, L., Lussi, Y. C., Vandamme, J., Riveiro, A. & Salcini, A. E. The H3K4me3/2
891 histone demethylase RBR-2 controls axon guidance by repressing the actin-remodeling gene
892 wsp-1. *Development* **143**, 851–863 (2016).

893 71. Nono, M. *et al.* Intestine-to-Germline Transmission of Epigenetic Information
894 Intergenerationally Ensures Systemic Stress Resistance in C. elegans. *Cell Rep.* **30**, 3207-
895 3217.e4 (2020).

896 72. Wani, K. A., Goswamy, D. & Irazoqui, J. E. Nervous system control of intestinal host
897 defense in C. elegans. *Curr. Opin. Neurobiol.* **62**, 1–9 (2020).

898 73. Sellegounder, D., Yuan, C.-H., Wibisono, P., Liu, Y. & Sun, J. Octopaminergic Signaling
899 Mediates Neural Regulation of Innate Immunity in Caenorhabditis elegans. *mBio* **9**, e01645-18
900 (2018).

901 74. Reddy, K. C., Andersen, E. C., Kruglyak, L. & Kim, D. H. A Polymorphism in npr-1 Is a
902 Behavioral Determinant of Pathogen Susceptibility in C. elegans. *Science* **323**, 382–384 (2009).

903 75. Styer, K. L. *et al.* Innate Immunity in Caenorhabditis elegans Is Regulated by Neurons
904 Expressing NPR-1/GPCR. *Science* **322**, 460–464 (2008).

905 76. Fruyt, N. D., Yu, A. J., Rankin, C. H., Beets, I. & Chew, Y. L. The role of neuropeptides in
906 learning: Insights from C. elegans. *Int. J. Biochem. Cell Biol.* **125**, 105801 (2020).

907 77. Gøtzsche, C. R. & Woldbye, D. P. D. The role of NPY in learning and memory.
908 *Neuropeptides* **55**, 79–89 (2016).

909 78. Pleil, K. E. *et al.* NPY signaling inhibits extended amygdala CRF neurons to suppress binge
910 alcohol drinking. *Nat Neurosci* **18**, 545–552 (2015).

911 79. Zhou, Z. *et al.* Genetic variation in human NPY expression affects stress response and
912 emotion. *Nature* **452**, 997–1001 (2008).

913 80. Naveilhan, P. *et al.* Normal feeding behavior, body weight and leptin response require the
914 neuropeptide Y Y2 receptor. *Nat Med* **5**, 1188–1193 (1999).

915 81. Cohen, H. *et al.* The Neuropeptide Y (NPY)-ergic System is Associated with Behavioral
916 Resilience to Stress Exposure in an Animal Model of Post-Traumatic Stress Disorder.
917 *Neuropsychopharmacol* **37**, 350–363 (2012).

918 82. Cohen, M. *et al.* Coordinated Regulation of Foraging and Metabolism in C. elegans by
919 RFamide Neuropeptide Signaling. *Cell Metab* **9**, 375–385 (2009).

920 83. Bhardwaj, A., Pandey, P. & Babu, K. Control of Locomotory Behavior of Caenorhabditis
921 elegans by the Immunoglobulin Superfamily Protein RIG-3. *Genetics* **214**, 135–145 (2020).

922 84. Lemieux, G. A. *et al.* Kynurenic Acid Is a Nutritional Cue that Enables Behavioral Plasticity.
923 *Cell* **160**, 119–131 (2015).

924 85. Choi, M.-K., Liu, H., Wu, T., Yang, W. & Zhang, Y. NMDAR-mediated modulation of gap
925 junction circuit regulates olfactory learning in C. elegans. *Nat. Commun.* **11**, 3467 (2020).

926 86. Hilbert, Z. A. & Kim, D. H. Sexually dimorphic control of gene expression in sensory
927 neurons regulates decision-making behavior in C. elegans. *Elife* **6**, 386 (2017).

87. Flavell, S. W. *et al.* Serotonin and the neuropeptide PDF initiate and extend opposing behavioral states in C. elegans. *Cell* **154**, 1023–1035 (2013).

88. Mukhopadhyay, S., Lu, Y., Shaham, S. & Sengupta, P. Sensory Signaling-Dependent Remodeling of Olfactory Cilia Architecture in C. elegans. *Dev. Cell* **14**, 762–774 (2008).

89. Komatsu, H., Mori, I., Rhee, J.-S., Akaike, N. & Ohshima, Y. Mutations in a Cyclic Nucleotide–Gated Channel Lead to Abnormal Thermosensation and Chemosensation in C. elegans. *Neuron* **17**, 707–718 (1996).

90. Yang, W. *et al.* Redundant neural circuits regulate olfactory integration. *Plos Genet* **18**, e1010029 (2022).

91. Sammut, M. *et al.* Glia-derived neurons are required for sex-specific learning in C. elegans. *Nature* **526**, 385–390 (2015).

92. Gutiérrez-Menéndez, A., Méndez, M. & Arias, J. L. Learning and metabolic brain differences between juvenile male and female rats in the execution of different training regimes of a spatial memory task. *Physiol Behav* **267**, 114203 (2023).

93. Rama, S., Zbili, M. & Debanne, D. Signal propagation along the axon. *Curr. Opin. Neurobiol.* **51**, 37–44 (2018).

94. Morais, L. H., Schreiber, H. L. & Mazmanian, S. K. The gut microbiota–brain axis in behaviour and brain disorders. *Nat Rev Microbiol* **19**, 241–255 (2021).

95. Hamson, D. K., Roes, M. M. & Galea, L. A. M. Comprehensive Physiology. *Compr. Physiol.* **6**, 1295–1337 (2017).

96. Frick, K. M., Kim, J., Tuscher, J. J. & Fortress, A. M. Sex steroid hormones matter for learning and memory: estrogenic regulation of hippocampal function in male and female rodents. *Learn. Mem.* **22**, 472–493 (2015).

97. Ernst, D. A., Agcaoili, G. A., Merrill, A. N. & Westerman, E. L. A learning experience elicits sex-dependent neurogenomic responses in Bicyclus anynana butterflies. *Mol Ecol* (2023) doi:10.1111/mec.16920.

98. Kilpatrick, Z. P., Davidson, J. D. & Hady, A. E. Uncertainty drives deviations in normative foraging decision strategies. *J Roy Soc Interface* **18**, 20210337 (2021).

99. Wu, T. *et al.* Pathogenic bacteria modulate pheromone response to promote mating. *Nature* **613**, 324–331 (2023).

100. Manning, T. H., Austin, M. W., MuseMorris, K. & Dunlap, A. S. Equivalent learning, but unequal participation: Male bumble bees learn comparably to females, but participate in cognitive assessments at lower rates. *Behav Process* **193**, 104528 (2021).

961 101. Wolf, S. & Chittka, L. Male bumblebees, Bombus terrestris, perform equally well as
962 workers in a serial colour-learning task. *Anim Behav* **111**, 147–155 (2016).

963 102. Lee, K. & Portman, D. S. Neural sex modifies the function of a C. elegans sensory circuit.
964 *Current Biology* **17**, 1858–1863 (2007).

965 103. Chronis, N., Zimmer, M. & Bargmann, C. I. Microfluidics for in vivo imaging of neuronal
966 and behavioral activity in Caenorhabditis elegans. *Nature Methods* **4**, 727–731 (2007).

967 104. Kohen, R. *et al.* UTAP: User-friendly Transcriptome Analysis Pipeline. *BMC Bioinform.*
968 **20**, 154 (2019).

969 105. Ge, S. X., Jung, D. & Yao, R. ShinyGO: a graphical enrichment tool for animals and plants.
970 *Bioinformatics* **36**, 2628–2629 (2019).

971 106. Paix, A., Folkmann, A., Rasoloson, D. & Seydoux, G. High Efficiency, Homology-Directed
972 Genome Editing in Caenorhabditis elegans Using CRISPR-Cas9 Ribonucleoprotein Complexes.
973 *Genetics* **201**, 47–54 (2015).

974 107. Hobert, O. PCR fusion-based approach to create reporter gene constructs for expression
975 analysis in transgenic C. elegans. *BioTechniques* **32**, 728–730 (2002).

976 108. Ahringer, J. Reverse genetics. *WormBook* 1–43 (2006) doi:10.1895/wormbook.1.47.1.

977

978